Australian Government
Department of Defence
Defence Science and
Technology Organisation

Smoothed Particle Hydrodynamics: Applications within DSTO

D.A. Jones and D. Belton

Maritime Platforms Division
Defence Science and Technology Organisation

DSTO-TR-1922

ABSTRACT

Smoothed Particle Hydrodynamics (SPH) is a computational technique for the numerical simulation of the equations of fluid dynamics without the use of an underlying numerical mesh. Although originally developed for use in astrophysical gas dynamics, SPH has recently been applied to many other areas of numerical fluid dynamics and materials modelling, several of which have particular relevance to defence problems of interest to the DSTO. In this report we review the basics of the method and then describe a simple two-dimensional SPH code for the simulation of incompressible fluid flow. The code is then applied to simple problems such as a dam break, the sloshing of water and wave breaking over ships. These examples illustrate both the capabilities of the technique and the relative ease with which the method can treat problems which have previously been considered difficult to solve using traditional methods such as finite difference, finite volume or finite element grid based methods. Further applications of the method are then reviewed, concentrating in particular on the utility of the technique in solid mechanics modelling, and then current applications of SPH within Maritime Platforms Division are described.

RELEASE LIMITATION

Approved for public release

APPROVED FOR PUBLIC RELEASE

Smoothed Particle Hydrodynamics: Applications within DSTO

Executive Summary

Smoothed Particle Hydrodynamics (SPH) is a computational technique for the numerical simulation of the equations of fluid dynamics without the use of an underlying numerical mesh. Although originally developed for use in astrophysical gas dynamics, SPH has recently been applied to many other areas of numerical fluid dynamics and materials modelling, several of which have particular relevance to defence problems of interest to the DSTO. In this report we review the basics of the method and then describe a simple two-dimensional SPH code for the simulation of incompressible fluid flow. The code is then applied to simple problems such as a dam break, the sloshing of water and wave breaking over ships. These examples illustrate both the capabilities of the technique and the relevant ease with which the method can treat problems which have previously been considered difficult to solve using traditional methods such as finite difference, finite volume or finite element grid based methods.

We then review the applications of SPH in solid mechanics modelling. Examples of this type of work which are of interest to the defence community include deformation due to high-velocity impact, the fracture and fragmentation of cased explosives, the formation and penetration of shaped charge jets, and debris cloud dynamics due to hypervelocity impact. SPH offers a new method with unique capabilities for the solution of such problems. We first discuss the application of SPH itself to these problems, then a hybrid approach which combines the best features of a Lagrangian finite element approach with the SPH method. This combined approach offers a significantly improved capability for the simulation of problems such as ballistic impact on confined and unconfined ceramic targets and transparent armour.

A summary is then given of relevant areas of work in Maritime Platforms Division where SPH methods are currently being used. These include the relative motion of a landing craft and the mother ship in a well dock scenario, sloshing within hulls, underwater explosion events, the deployment and retrieval of autonomous vehicles, and ballistic impact on ceramic targets.

Authors

David A. Jones
Maritime Platforms Division

Dr. David A. Jones obtained a B.Sc. (Hons) and Ph.D. in Theoretical Physics from Monash University in 1973 and 1976 respectively. He joined the then Materials Research Laboratories in 1983 after postdoctoral positions at the University of Strathclyde, Glasgow; Queen Mary College, London University, and the University of New South Wales, Sydney. During 1987/88 he was a visiting scientist at the Laboratory for Computational Physics and Fluid Dynamics at the Naval Research Laboratory, Washington, DC. He has authored 80 journal articles and technical reports and given more than 60 presentations at scientific meetings. His research has covered a variety of areas including polymer dynamics, the application of chaos theory to atomic and molecular physics, laser-plasma interaction theory, warhead design, air blast, detonation physics and computational fluid dynamics.

Daniel Belton
Maritime Platforms Division

Daniel Belton graduated from Monash University, Clayton, in 2004 with a Bachelor of Science (Hons) and Bachelor of Engineering (Hons) degree. He completed a Science Honours thesis on applying SPH to tsunami inundation on a vegetated coast under Prof. Joe Monaghan, and an engineering final year project on; "Stochastic analysis of vehicle crash performance." Daniel joined the Maritime Platform Division of DSTO in 2005, working in areas of structural mechanics and engine control systems.

Contents

1. Introduction

Smoothed Particle Hydrodynamics (SPH) was developed independently by Gingold and Monaghan [20] and Leon Lucy [45] in 1977 to simulate astrophysical gas dynamics problems. The many techniques available at that time for the numerical solution of the compressible fluid dynamic equations were often unsuitable for astrophysical applications. There were several reasons for this; astrophysical problems often involve large changes in spatial, temporal and density scales over many orders of magnitude. Such problems are also often inherently asymmetric and have no definite boundaries. A typical example from astrophysics which illustrates these problems is the numerical simulation of the fission of a rapidly rotating star.

Traditional techniques for the numerical solution of hydrodynamic equations first involve the creation of a computational mesh which is used to discretise the partial differential equations describing the flow. The partial derivatives can be approximated by a number of different methods including finite difference, finite volume, or finite element schemes. The computational mesh can be either fixed in space and cover the entire fluid domain (the Eulerian method), or can be fixed to the fluid and move with the flow (the Lagrangian method). The Eulerian method often requires the construction of a very fine mesh over the whole flow domain because the location of the interesting features of the flow is not known *a priori*. Hence the method is often computationally expensive. Fixed grid methods can also suffer from excessive numerical diffusion due to the non-linear convective terms which arise in the Eulerian description of the flow.

Lagrangian meshes overcome these problems by attaching the mesh points to the fluid itself and allowing the points to move with the flow. The non-linear terms then no longer appear and the mesh need only be defined in the regions of space occupied by the fluid. If the motion of the fluid becomes geometrically complex however then the mesh undergoes severe distortion and the underlying numerical methods become unstable and the computation stops.

Neither of these approaches is particularly suited to astrophysical fluid problems due to the lack of symmetry, complex rotational behaviour and range of spatial scales inherent in many of these problems. SPH was developed to provide a computational scheme for the solution of the fluid equations which did not rely on the use of a computational mesh. This is achieved by defining a set of moving interpolation points which follow the fluid motion. In this sense SPH is a Lagrangian method, although the points are never linked together to create a computational mesh. Each of the fluid dynamic variables is expressed as an integral interpolant using a smoothing function and the integral is then approximated by a summation over the interpolation points. By using this approach, the derivatives of the fluid variables can then be evaluated by calculating the derivatives of the smoothing function.

Although originally developed for use in astrophysical gas dynamics, the many advantages inherent in the absence of a computational mesh have resulted in SPH being adapted and applied to many other areas of numerical fluid dynamics and materials modelling. Typical applications include, free surface flow, high velocity impact, material fracture, detonation physics, plasma dynamics, marine fluid-structure interactions, and

geophysical fluid flows. Many of these areas of application are relevant to research currently undertaken by scientists in both the Maritime Platforms Division (MPD) and the Weapons System Division (WSD) of DSTO.

The extent of development and application of SPH to the many diverse areas of fluid flow and solids modelling is such that no review of SPH can hope to cover each area of application in detail. The purpose of this report is to provide a simple introduction to the basics of SPH, to review in some detail those areas of application of most relevance to MPD and WSD, and to report simulation results from selected two-dimensional calculations which were performed to emphasize the attractiveness and simplicity of the method when applied to problems which have previously been considered difficult to solve using traditional techniques such as finite difference, finite volume or finite element grid based methods.

2. SPH – The Basics

In this section we briefly outline the basis of the SPH method and illustrate the derivation of the fluid dynamic equations in SPH form. A number of review articles which describe the foundations of the method have already been written. A relatively short paper written by Monaghan in 1988 gives a clear derivation of the SPH equations and describes their application to a wide variety of problems in compressible flow [51]. A more detailed and lengthy review of the method in connection with astrophysical gas dynamics appeared several years later [53]. More recently, Monaghan has written a very comprehensive review which details the theory and application of SPH since its inception in 1977 [55]. As well as a detailed review of the foundations of the subject Monaghan also describes recent applications of SPH in areas such as incompressible fluid flow, fluid-structure interactions, turbulence, heat conduction, elasticity and fracture. Benz has also written several review articles which outline the basis of the method and its applications in astrophysics [2,3] and brittle solids modelling [4]. The recent book by Liu and Liu [43] provides a very extensive review of the foundations of the subject as well as providing many illustrations of the application of the method to the simulation of detonation, underwater explosion shocks, and the hydrodynamics of material strength.

2.1 Integral Interpolants

The basis of SPH is the expression of each of the fluid dynamic variables as an integral interpolant. This allows any function to be expressed in terms of its values at a set of disordered points. Consider a general function A($\mathbf{r}$) expressed in the form

$$A(\mathbf{r}) = \int A(\mathbf{r}')\delta(\mathbf{r} - \mathbf{r}')\mathbf{dr}' \qquad (1)$$

where $\delta(\mathbf{r} \text{ - } \mathbf{r}')$ is the Dirac delta function and the integral is taken over the entire three-dimensional space. Equation (1) is exact, but not particularly useful. The basic idea of SPH is to approximate the delta function by a suitable continuous function. In SPH this function is called the kernel, and the choice of a suitable kernel is of central importance to the success of the SPH method.

The integral interpolant $\langle A(\mathbf{r}) \rangle$ of any function A($\mathbf{r}$) is defined as

$$\langle A(\mathbf{r}) \rangle = \int A(\mathbf{r}')W(\mathbf{r} - \mathbf{r}', h)\mathbf{dr}' \qquad (2)$$

where the function W has the two properties:

$$\int A(\mathbf{r}')W(\mathbf{r} - \mathbf{r}', h)\mathbf{dr}' = 1 \qquad (3)$$

$$\lim_{h \to 0} W(\mathbf{r} - \mathbf{r}', h) = \delta(\mathbf{r} - \mathbf{r}') \qquad (4)$$

Lucy [45] referred to the function W as a broadening function because it spreads the influence of A on $\mathbf{r}$ to the surrounding region. The length scale h is effectively the half-width of the kernel and determines the amount of broadening, or the spatial extent over which the function W smoothes the variable A. This half-width is the resolution length scale of SPH and is referred to as the smoothing length. It is equivalent to the width of a grid-cell in finite difference methods.

Consider a fluid with density ρ($\mathbf{r}$) defined by a set of points $\mathbf{r}_i$ initially distributed in a regular manner throughout the body of the fluid. At any time the velocity and any other fluid dynamic variables are also known at these points. We can imagine the fluid to be divided into N small volume elements with masses m_1, m_2, ….., m_N, where the "centres" of these small volumes are located at the $\mathbf{r}_i$. Evidently $\rho(\mathbf{r}_i)\mathbf{dr} = m_i$, hence for numerical simulations the integral interpolant $\langle A(\mathbf{r}) \rangle$ can be approximated as follows:

$$\langle A(\mathbf{r}) \rangle = \int \frac{A(\mathbf{r}')}{\rho(\mathbf{r}')} W(\mathbf{r} - \mathbf{r}', h)\rho(\mathbf{r}')\mathbf{dr}'$$

$$\langle A(\mathbf{r}) \rangle \approx \sum_{i=1}^{N} m_i \frac{A_i}{\rho_i} W(\mathbf{r} - \mathbf{r}', h) \qquad (5)$$

where the summation index i denotes a particle label and the summation is over all N particles. Particle i has mass m_i, position $\mathbf{r}_i$, density ρ_i and velocity $\mathbf{v}_i$. The value of any variable A at $\mathbf{r}_i$ is denoted by A_i.

The particular advantage of the SPH formulation becomes apparent when we consider the integral interpolant expression for the gradient of a function

$$\langle \nabla A(\mathbf{r}) \rangle = \int \nabla A(\mathbf{r}')W(\mathbf{r} - \mathbf{r}', h)\mathbf{dr}' \qquad (6)$$

Integrating by parts, equation (6) becomes

$$\langle \nabla A(\mathbf{r}) \rangle = \int A(\mathbf{r}')\nabla W(\mathbf{r} - \mathbf{r}', h)\mathbf{dr}' + \int A(\mathbf{r}')W(\mathbf{r} - \mathbf{r}')n_{\mathbf{r}'}dS \qquad (7)$$

The first integral on the right side of equation (7) is taken over the volume of the domain, while the second integral is over the boundary of the domain. In most applications this surface integral can be neglected because either the function or the kernel itself goes to zero at the boundary of the domain. Equation (7) therefore becomes

$$\langle \nabla A(\mathbf{r}) \rangle = \int A(\mathbf{r}') \nabla W(\mathbf{r} - \mathbf{r}', h) \mathbf{dr}' \qquad (8)$$

which in numerical terms becomes

$$\nabla A(\mathbf{r}) = \sum_i m_i \frac{A_i}{\rho_i} \nabla W(\mathbf{r} - \mathbf{r}_i, h) \qquad (9)$$

Equation (9) displays the fundamental advantage of the SPH method; that the derivatives of any function A(**r**) can be found by differentiating the kernel, rather than by using finite difference, finite volume or finite element expressions calculated from a grid.

The error involved in approximating the function A(**r**) by the summation given by equation (5) has been studied in detail by Monaghan [49]. It depends on the degree of disorder of the particles, but generally is of O(h^2) or better. Monaghan has discussed this point in more detail in his most recent review [55], where he notes that it is not easy to estimate the errors in the SPH equations from first principles because the particles get disordered during motion. The degree of disorder is not complete however, as would be described by a probability distribution proportional to the mass density for example, because the particles are still constrained by the dynamics. Consequently, SPH simulations have been found to be much more accurate than the interpolation of quantities from randomly disordered particle arrays would suggest. It should also be noted that although the summation in equation (5) is formally over all the particles, only a small number actually contribute because W can be chosen so that it falls off rapidly for $|\mathbf{r} - \mathbf{r}_i| \geq h$.

From a mathematical point of view the points $\mathbf{r}_i$ with associated masses m_i are simply interpolation points from which the properties of the fluid can be calculated. From a physical point of view however the points can be regarded as material particles with masses m_i which can be treated like any other particle system. It is this physical interpretation of the SPH equations which is most universally adopted and allows SPH to provide a conceptually simple formulation in which the inclusion of more complicated physics is a relatively straightforward procedure.

2.2 Choice of kernel function

The original calculations of Gingold and Monaghan [20] used a Gaussian kernel, while those of Lucy [45] used a bell-shaped function constructed from a third order polynomial. Many other functions are possible however, and Liu and Liu [43] give a detailed discussion of the main properties which any kernel function should satisfy, and also provide a comprehensive list of some of the most frequently used functions in the SPH literature.

By far the most popular kernel function is the one devised by Monaghan and Lattanzio [60] based on cubic spline functions:

$$W(q, \mathrm{h}) = \frac{\sigma}{h^\nu} \left\{ 1 - \frac{3}{2} q^2 + \frac{3}{4} q^3 \right\} \qquad \text{if } 0 \leq q \leq 1$$

$$= \frac{\sigma}{h^{\nu}} \frac{1}{4} \{2 - q\}^3 \qquad\qquad \text{if } 1 \le q \le 2$$
$$= 0 \qquad\qquad\qquad\qquad \text{if } q > 2 \qquad\qquad (11)$$

where ν is the number of dimensions and σ is a normalisation constant which takes the values $2/3$, $10/7\pi$ and $1/\pi$ in one, two and three dimensions respectively. This function closely resembles the original Gaussian function used by Gingold and Monaghan [20], but has the advantage of having compact support (meaning that the interactions are exactly zero for $r > 2h$) and a continuous second derivative. The vanishing of the kernel for $r > 2h$ is particularly important because it means that the summation in equation (5) needs to be carried out only for particles within a radius of $2h$ of the point of interest.

Some of the other functions described in the literature include both quartic and quintic spline expressions introduced by Morris [61], which more closely approximate a Gaussian shape and are more stable. Johnson et al. [36] used a quadratic smoothing function because it was found to overcome a compressive instability problem which occurs in high velocity impact problems. Liu and Liu [43] recently introduced a new kernel based on a fourth order polynomial expression which gives excellent results in the standard shock tube problem and in two-dimensional heat conduction simulations.

2.3 Equations of motion in SPH form

The original SPH equations were derived to simulate astrophysical gas dynamic problems. The momentum equation, in Lagrangian form, neglecting the effects of viscosity and gravity therefore takes the form

$$\frac{d\mathbf{v}}{dt} = -\frac{1}{\rho} \nabla P \qquad\qquad (12)$$

It is assumed that the fluid has an equation of state in which the pressure P is a function of the density ρ only. From equation (5) we can then express the pressure gradient as

$$\nabla P = \sum_b m_b \frac{P_b}{\rho_b} \nabla W(\mathbf{r} - \mathbf{r}_b, h) \qquad\qquad (13)$$

where we now denote a particle label by the summation index b. Hence equation (12) can be written in SPH form as

$$\frac{d\mathbf{v}_a}{dt} = -\frac{1}{\rho_a} \sum_b m_b \frac{P_b}{\rho_b} \nabla_a W_{ab} \qquad\qquad (14)$$

where we now employ the standard SPH practice of referring to the interpolation points as particles and equation (14) is interpreted as the force on particle a due to all other particles b in the region of particle a. ∇_a implies taking the gradient with respect to the coordinates of particle a. and we have now introduced the standard notation $W_{ab} = W(\mathbf{r}_a - \mathbf{r}_b, h)$.

To this we need to add an equation describing the motion of the particles at each time step

$$\frac{d\mathbf{r}_a}{dt} = \mathbf{v}_a \qquad (15)$$

From equation (5) it is also obvious that the equation for the density at any point is given by

$$\rho_a = \sum_b m_b W_{ab} \qquad (16)$$

Whilst the above equations look reasonable and are the forms used in the original papers by Gingold and Monaghan [20] and Lucy [45], they are usually modified slightly to produce better results. Equation (14) for example does not conserve linear and angular momentum exactly because the force on particle a due to particle b is not equal to the force on particle b due to particle a. The forces can be made symmetrical by first writing $\nabla P / \rho$ in the form

$$\frac{\nabla P}{\rho} = \nabla\left(\frac{P}{\rho}\right) + \frac{P}{\rho^2}\nabla\rho \qquad (17)$$

and then applying the SPH interpolation rules so that the momentum equation becomes

$$\frac{d\mathbf{v}_a}{dt} = -\sum_b m_b \left(\frac{P_b}{\rho_b^2} + \frac{P_a}{\rho_a^2}\right)\nabla_a W_{ab} \qquad (18)$$

This form of the momentum equation conserves linear and angular momentum exactly. It was first derived by Gingold and Monaghan using a different approach [22,23,24].

Two further modifications are particularly relevant when SPH is used to simulate the motion of fluids, which is the case in the simulations described in this report. Instead of moving the particles according to equation (15), their motion is described by

$$\frac{d\mathbf{r}_a}{dt} = \mathbf{v}_a + \varepsilon \sum_b m_b \left(\frac{\mathbf{v}_{ba}}{\overline{\rho}_{ab}}\right)W_{ab} \qquad (19)$$

where $\overline{\rho}_{ab} = (\rho_a + \rho_b)/2$, $\mathbf{v}_{ba} = \mathbf{v}_b - \mathbf{v}_a$, and ε is a constant with a value normally of ½. Equation (19) is known as the XSPH variant and was introduced by Monaghan [52] to prevent penetration when particle methods are used to simulate streams of fluid impinging on each other. The additional term in equation (19) ensures that a particle moves with a velocity that is close to the average velocity in its neighbourhood. For the simulation of nearly incompressible fluids such as water it has been found to keep the particles orderly in the absence of viscosity.

For many SPH simulations the density is calculated from equation (16). For nearly incompressible flow with a free surface however, such as water sloshing in a tank, use of equation (16) produces incorrect results. In these types of problems the density falls discontinuously to zero at the surface. If equation (16) is used to find the density then the

particles near the surface will have their densities smoothed over a length 2*h*, hence the density will not drop discontinuously as it should. The resulting smoothing of the density discontinuity produces incorrect pressures and hence poor results near the surface, which in some applications is the main feature of interest. To overcome this problem, the continuity equation, i.e.

$$\frac{\partial \rho}{\partial t} + \nabla \cdot (\rho \mathbf{v}) = 0 \tag{20}$$

can be expressed in SPH form as follows

$$\frac{d\rho_a}{dt} = \sum_b m_b \mathbf{v}_{ab} \cdot \nabla_a W_{ab} \tag{21}$$

By using equation (21) instead of equation (16) the initial density can be set and then it will only change when particles move relative to each other. There is also a computational advantage to using equation (21) in place of equation (16) since the rate of change of all physical variables can then be computed in one computational loop.

2.4 Inclusion of viscosity

Although Lucy [45] was the first to introduce a viscosity term in the SPH equations, the most widely used expression for viscosity in SPH simulations was introduced by Monaghan and Gingold [57]. It should be noted that any numerical simulation of the hydrodynamic equations which involve supersonic motions and the formation of shocks, whether grid based or not, requires some form of viscosity to stabilize the shock. The viscosity term introduced by Monaghan and Gingold [57] has the advantage of containing a term linear in velocity, which produces a representation of the classical shear and bulk viscosities, as well as a quadratic velocity term which handles high Mach number shocks and is the SPH equivalent to the Von Neumann-Richtmeyer artificial viscosity used in finite-difference methods.

To understand the form of the viscosity term as introduced by Monaghan and Gingold we first consider the Navier-Stokes equation for viscous fluids

$$\frac{d\mathbf{v}}{dt} = -\frac{1}{\rho}\nabla P + \frac{\mu}{\rho}\nabla^2 \mathbf{v} \tag{22}$$

where μ is the coefficient of viscosity. Note that the addition of viscosity adds a second derivative term to the equation. In principle this is not a problem, as second derivatives can be estimated by differentiating the SPH interpolant twice. In practice however the expression can be very sensitive to particle disorder. To avoid this potential problem Monaghan and Gingold took a different approach. Equation (22) can be written in the following form

$$\frac{d\mathbf{v}}{dt} = -\frac{1}{\rho}\nabla\{P - \mu\nabla\mathbf{v}\} \tag{23}$$

7

which shows that the viscosity can be regarded as an extra pressure term. Using this analogy, Monaghan and Gingold took the SPH version of the Navier-Stokes equation to have the form

$$\frac{d\mathbf{v}_a}{dt} = -\sum_b (\frac{P_b}{\rho_b^2} + \frac{P_a}{\rho_a^2} + \Pi_{ab})\nabla_a W_{ab} \tag{24}$$

where Π_{ab} is the additional "viscous pressure" term. Comparing equations (22) and (23) it is obvious that Π should have the form

$$\Pi \approx \frac{\mu}{\rho^2}\nabla|\mathbf{v}| \tag{25}$$

Now for a gas, the coefficient of viscosity μ is given approximately by

$$\mu \approx \rho\lambda c \tag{26}$$

where λ is the mean-free path length of the gas molecules and c is the speed of sound in the gas. The logical extension of this form of the coefficient of viscosity to SPH is simply to replace λ with h. Consider the case of one-dimensional motion first for simplicity. The need to take a second derivative of the interpolant can be overcome by expressing the velocity derivative in equation (25) by a simple finite difference form

$$\frac{d\mathbf{v}}{d\mathbf{x}} \approx \frac{\mathbf{v}_a - \mathbf{v}_b}{\mathbf{x}_a - \mathbf{x}_b} \tag{27}$$

Combining equations (25), (26) and (27) the expression for Π_{ab} (in one-dimension) becomes

$$\Pi_{ab} = -\left(\frac{\alpha h c_a}{\rho_a}\right)\left(\frac{\mathbf{v}_a - \mathbf{v}_b}{\mathbf{x}_a - \mathbf{x}_b}\right) \tag{28}$$

where α is a dimensionless coefficient which can be used to fine tune the expression for a particular simulation. To conserve momentum however Π_{ab} needs to be symmetric, so c_a and ρ_a are replaced by the symmetrised forms $\bar{c}_{ab}$ and $\bar{\rho}_{ab}$, where $\bar{c}_{ab} = (c_a + c_b)/2$ and $\bar{\rho}_{ab} = (\rho_a + \rho_b)/2$. To avoid a problem when $|\mathbf{v}_{ab}| \neq 0$ and $\mathbf{x}_{ab}$ approaches zero $\mathbf{v}_{ab}/\mathbf{x}_{ab}$ is replaced as follows

$$\frac{\mathbf{v}_{ab}}{\mathbf{x}_{ab}} = \frac{\mathbf{v}_{ab}\mathbf{x}_{ab}}{x_{ab}^2 + \eta^2} \tag{29}$$

where $\eta^2 = 0.001h^2$. Generalizing to three dimensions the expression for Π_{ab} then becomes

$$\Pi_{ab} = -\left(\frac{\alpha h \overline{c}_{ab}}{\overline{\rho}_{ab}}\right)\left(\frac{\mathbf{v}_{ab} \bullet \mathbf{r}_{ab}}{r_{ab}^2 + \eta^2}\right) \tag{30}$$

Equation (30) successfully reproduces the linear shear and bulk viscosity of fluids and was also found to stabilize shocks of moderate strength [57]. For astrophysical problems involving colliding gas clouds however problems still persisted and so an extra term was added. The additional term is quadratic in velocity and is the SPH equivalent of the Von Neumann-Richtmeyer artificial viscosity used in finite-difference methods. The complete expression for the general viscosity term Π_{ab} then takes the form

$$\Pi_{ab} = -\frac{\alpha \overline{c}_{ab} \mu_{ab} + \beta \mu_{ab}^2}{\overline{\rho}_{ab}} \tag{31}$$

where

$$\mu_{ab} = \frac{h \mathbf{v}_{ab} \bullet \mathbf{r}_{ab}}{r_{ab}^2 + \eta^2}$$

When simulating high Mach number compressible gas flows where the real viscosity is negligible then equation (31) only applies when the fluid is being compressed, i.e. when particles are approaching one another, which is the condition $\mathbf{v}_{ab} \bullet \mathbf{r}_{ab} < 0$. When $\mathbf{v}_{ab} \bullet \mathbf{r}_{ab} > 0$ the gas is expanding and then $\Pi_{ab} = 0$. In many applications to high speed flow it has been found that the choice of $\alpha = 1$ and $\beta = 2$ produces excellent results.

In the opposite extreme of low Mach number flows where the fluid has significant real viscosity then equation (31) can be used with $\beta = 0$. The value of α is then chosen so that the simulated fluid has a viscosity and Reynolds number similar to that of the real fluid being modelled. By performing a more careful analysis of equation (31) Monaghan and Kos [58] have shown that it leads to a shear viscosity of the form

$$\mu = \frac{1}{8}\alpha h c \rho \tag{32}$$

Monaghan [54] has used equation (31) with $\beta = 0$ and $\alpha = 0.01$ to simulate the evolution of an elliptical water drop, the bursting of a dam, and the formation of a bore and in each case has found excellent agreement with experimental results. Monaghan and Kos [58] also used equation (31) with $\beta = 0$ and $\alpha = 0.001$ to simulate the run-up and return of a solitary wave travelling over shallowing water and then onto a dry beach backed by a vertical wall. The simulations accurately reproduced the experimental results. Equation (31) was used to reproduce the effects of viscosity in all the simulations reported in Section 3 of this report.

Whilst equation (31) has been shown to give accurate results in many scenarios, including typical fluid flows of interest in MPD, Morris et al. [62] found that it gave inaccurate velocity profiles in their simulations of Couette and Poiseuille flow when the Reynolds number was $O(10^{-2})$. They overcame this problem by using an expression similar to the first term in equation (31) but based on an SPH estimation of viscous diffusion which is

similar to an expression used to model heat conduction. Their hybrid expression still combined a standard SPH first derivative with a finite difference approximation of a first derivative. Takeda et al. [74] were the first to use second-order derivatives of the kernel to represent the second-order derivatives in the expression for the viscous term in the Navier-Stokes equation. They calculated isothermal viscous flow around a cylinder for Reynolds numbers in the range $6 \leq Re \leq 55$ and found excellent agreement with results calculated using standard finite difference methods. Watkins et al. [76] have shown how to use standard SPH expressions for first derivatives to calculate accurate expressions for the viscous term in the Navier-Stokes equation using only first derivatives of the kernel. They conducted a series of tests on problems for which analytical solutions exist and found excellent agreement with the theoretical solutions.

Balsara [1] has noted that the use of equation (31) leads to substantial spurious entropy generation in regions of strong shear. He solved this problem by multiplying μ_{ab} by a suitably devised function of the local compression and vorticity which approached unity in regions of strong compression and zero in regions of strong vorticity. Calagrossi and Landrini [11] slightly modified Balsara's correction term and used it in a number of simulations of the classical dam break problem. They found that this improved the quality of the solution both for free surface and interfacial flows, and also improved total energy conservation.

For SPH simulations involving two or more fluids with very different viscosities Cleary [8] has used a more sophisticated viscous term than that given by equation (31) which allows the viscosity to be variable and ensures that stress is automatically continuous across material interfaces. Cleary et al. [9] have shown that this form of the viscosity allows multiple materials with densities and viscosities varying by up to three orders of magnitude to be accurately simulated

2.5 Treating incompressible fluids

The development of SPH outlined so far assumes that the fluid is compressible. Since water is an almost incompressible fluid some modifications are required if SPH is to be used for hydrodynamic simulations. Monaghan showed how this could be achieved in 1994 [54]. Since the speed of sound in water is of the order of 10^3 m/s the Mach number in typical simulations is extremely small. It is therefore customary in typical finite difference, finite volume or finite element grid based methods to approximate the fluid by an artificial fluid which is exactly incompressible. In SPH simulations the opposite approach is taken; the real fluid is approximated by an artificial fluid which is more compressible than the real fluid. The artificial fluid will still provide a valid approximation to the motion of the real fluid provided that the speed of sound is still much larger than the speed of the bulk flow. Because relative density fluctuations are proportional to M^2 (where M is the Mach number), density fluctuations can be limited to $\sim 1\%$ provided $M \sim 0.1$. This means that the standard SPH formulation described above can still be used. The only modification required is to change the equation of state of the (nearly incompressible) fluid so that the material becomes more compressible, while retaining sufficient incompressibility so that the speed of sound is large enough to keep the relative density fluctuations small.

A standard equation of state which is used for water in many hydrodynamic simulations is the one due to Cole [12], which can be written in the form

$$P = B\left(\left(\frac{\rho}{\rho_0}\right)^n - 1\right)$$

(33)

where P and the constant B are measured in atmospheres and ρ_0 is the density at atmospheric pressure. When n and B take the values 7 and 3,000 respectively this equation agrees with the data for water to within a few percent for pressures less than 10^5 atmospheres. Monaghan has used this equation of state to successfully simulate the flow of elliptical drops of water, bursting dams, the formation of bores, and waves on a beach [58]. The only modification to the equation of state required was to change the value of the constant B. With the equation of state given by equation (33) the speed of sound c at the reference density ρ_0 is given by

$$c^2 = \frac{n\mathrm{B}}{\rho_0}$$

(34)

Therefore, if B = $100\rho_0 v^2/n$, the relative density fluctuations should be ~ 0.01. This simply requires that an estimate of the maximum flow speed needs to be made for each new problem. A simple example is a dam of height H collapsing. An approximate upper bound on the speed of the water is then given by $v^2 = 2gH$, where g is the strength of the gravitational constant.

2.6 Inclusion of boundaries

Most boundary methods in SPH involve the use of boundary particles which apply forces on the fluid particles. The general form of this force is to treat the boundary force as if it were a molecular force. The force is then directed centrally between the particles and has the Lennard-Jones form

$$f(r) = D\left(\left\{\frac{r_0}{r}\right\}^{p1} - \left\{\frac{r_0}{r}\right\}^{p2}\right)\frac{\mathbf{r}}{r^2}$$

(35)

but is set to zero if $r > r_0$ so that the force is purely repulsive. The constants p_1 and p_2 must satisfy the condition $p_1 > p_2$ and typically have the values $p_1 = 4$ and $p_2 = 2$, although similar results are found using $p_1 = 12$ and $p_2 = 6$. The length scale r_0 is taken to be the initial spacing between the particles and the coefficient D (which has dimensions of velocity squared) is again chosen by considering a typical speed in the problem. For example, for problems involving dams, bores or weirs with fluid of depth H Monaghan has used D = $5gH$, but has also shown that simulations using D = $10gH$ or D = gH give similar results [54].

Equation (35) was used by Monaghan in his initial free surface flow simulations [54] and favourable results were obtained. The method is not ideal however as it produces the

equivalent of a corrugated boundary containing ripples on the scale of the particle spacing. Monaghan and Koss [58] developed a better approach which uses an interpolation procedure so that the forces from neighbouring boundary particles produce a force normal to the boundary. In this method boundary particles are assigned both a position and a local unit normal vector **n** that points from the boundary into the fluid. The force per unit mass **f** on a fluid particle from a boundary particle is computed using the components of their separation along the normal (denoted by y) and along the tangent (denoted by x), where the distances x and y are taken to be positive. The force then takes the form

$$\mathbf{f} = R(y)\,P(x)\,\mathbf{n} \tag{36}$$

where R(y) is designed to fall to zero within a few particle spacings of the wall. In terms of the variable q, where $q = y/(2\Delta p)$ (where Δp is the initial particle spacing), R(y) is defined by

$$R(y) = A \frac{1}{\sqrt{q}}(1-q) \quad \text{if } q < 1 \tag{37}$$

else R(y) = zero. The parameter A in equation (37) is given by the expression

$$A = \frac{1}{h}\left(0.01c^2 + \beta c\mathbf{v}_{ab} \bullet \mathbf{n}_b\right) \tag{38}$$

where the fluid particle is a and the boundary particle is b. β is 1 if the particles are approaching; otherwise it is zero. The second term in equation (38) helps damp-out the motion perpendicular to the boundary. The function P(x) is defined by

$$P(x) = \frac{1}{2}\left(1 + \cos\left\{\frac{\pi x}{\Delta p}\right\}\right) \quad \text{if } x < \Delta p \tag{39}$$

otherwise P(x) = zero. The function P(x) ensures that as a fluid particle moves between two boundary particles the contribution from the particles combines to make the boundary force constant if the fluid particle moves parallel to the boundary.

More recently Monaghan, Kos and Issa [59] have used different expressions for the functions R(y) and P(x). If q is now defined as $q = y/h$, the function R(y) is defined by

$$\begin{aligned} R(y) &= \frac{2}{3}\beta & \text{if } 0 < q < 2/3 \\[2mm] &= \beta\left(2q - \frac{3}{2}q^2\right) & \text{if } 2/3 < q < 1 \\[2mm] &= \frac{1}{2}\beta(2-q)^2 & \text{if } 1 < q < 2 \end{aligned} \tag{40}$$

and is zero for $q > 2$. The constant $\beta = 0.02c^2/y$ and is an estimate of the maximum force per unit mass necessary to stop a particle moving at the estimated maximum speed. The factor $1/y$ ensures that a particle moving faster than this can also be stopped. This new form for R(y) was chosen because the boundary force opposes the pressure gradient and R(y) has the form of the gradient of the kernel. The function P(x) is now simply defined by

$$P(x) = \left(1 - \frac{x}{\Delta p}\right) \qquad \text{if } 0{<}x{<}\Delta p \qquad (41)$$

and is zero otherwise. Monaghan et al. [59] have used the form of the boundary force defined by equations (40) and (41) in a study of the impact between a rigid body and water but have found that there is little difference between the results obtained using these expressions and the results obtained from equations (36) and (38). In Section 3 we describe the results obtained from SPH simulations using both versions of the boundary force and show that the results obtained are independent of the assumed form of this force.

Other approaches to the problem of specifying realistic boundary conditions are possible. Both Takeda et al. [74] and Morris et al. [62] performed simulations for low Reynolds numbers where the no-slip condition was the appropriate boundary condition. To achieve this they used "imaginary particles" outside the boundary surface. Libersky and Petschek [41] have used a similar approach where the additional particles are referred to as "ghost particles". Randles and Libersky [69] extended this approach to more general boundary conditions. These schemes work by regarding the boundary as a symmetrically reflecting interface, so that the imaginary particles have the same density and pressure as the corresponding real particles, but opposite velocity.

Liu and Liu [43] use two types of virtual particles to treat solid boundary conditions. Virtual particles of the first type are located right on the solid boundary and are similar to those used by Monaghan and described above. Virtual particles of the second type are similar to those used by Libersky and Petschek [41]. Liu and Liu found that both particle types were needed; the virtual particles of the first type ensured that the real particles were prevented from penetrating the boundaries, while the virtual particles of the second type were needed to impose the correct boundary conditions. The various schemes differ from one another in the exact methods used to calculate the velocities of the image particles, the degree to which these particles are carried along by the flow and are included in the summation process, and by the way in which the kernel sum is normalized.

In the simulations presented in Section 3 we have not used ghost particles nor any form of virtual or imaginary particles outside the boundary surface. We have used boundary particles as defined by Monaghan and Koss [58] and have included the boundary particles in the density calculation by solving the continuity equation in the form of equation (21). We note that if fluids of very different densities were present in the simulation then a different form of the continuity equation would be required.

2.7 Time stepping considerations

The SPH formulation of the equations of fluid dynamics reduces them to a set of ordinary differential equations for the motion of each of the particles within the simulation. Hence any numerical technique for the solution of coupled ordinary differential equations can be used for their solution. In practice however, the right hand side of the momentum equation for each particle, equation (14) or equation (18), is generally quite expensive in terms of computer time to evaluate and this tends to exclude schemes such as high order Runge-Kutta methods which require several evaluations of the force term at each time

step. Most SPH codes use either an improved Euler method (a mid-point predictor-corrector method) [50] or a leapfrog predictor-corrector algorithm for time stepping [51]. Each of these methods requires only one evaluation of the force term per time step.

In the code used to generate the results shown in the next section we used the predictor-corrector leapfrog algorithm for time stepping. If we write the set of equations describing the change in velocity, position and density in the following form

$$\frac{d\,\mathrm{v}_a}{dt} = F_a \tag{42}$$

$$\frac{d\,r_a}{dt} = \mathrm{v}_a \tag{43}$$

$$\frac{d\rho_a}{dt} = D_a \tag{44}$$

and denote the values of the variables at the beginning of a time step Δt by $\mathrm{v}_a{}^0$, $F_a{}^0$, $r_a{}^0$, $\rho_a{}^0$ and $D_a{}^0$ then the predictor step is given by

$$\mathrm{v}_{ap} = \mathrm{v}_a^0 + \Delta t\, F_a^0 \tag{45}$$

$$r_a = r_a^0 + \Delta t\, \mathrm{v}_a^0 + \frac{1}{2}(\Delta t)^2\, F_a^0 \tag{46}$$

$$\rho_{ap} = \rho_a^0 + \Delta t\, D_a^0 \tag{47}$$

New values of F_a and D_a are calculated using the predicted quantities and then corrected values of v_a and ρ_a are calculated according to

$$\mathrm{v}_a = \mathrm{v}_{ap} + \frac{1}{2}\Delta t\left(F_{ap} - F_a^0\right) \tag{48}$$

$$\rho_a = \rho_{ap} + \frac{1}{2}\Delta t\left(D_{ap} - D_a^0\right) \tag{49}$$

The time step is limited by the familiar CFL condition, which basically restricts the physical rate of propagation of information to be less than that of the numerical propagation rate. In SPH terms this becomes $\Delta t \le h/c$. If viscosity is present however this leads to an additional diffusive limitation on the time step and the two effects are usually combined in the following expression

$$\Delta t_{cv} = \min_a \frac{h}{c + 0.6(\alpha c + \beta \max_b \mu_{ab})} \tag{50}$$

A further limitation on the time step applies if external body forces are present. This implies that the time step should be less than Δt_f, where $\Delta t_f = (h/|\mathbf{f}|)^{1/2}$ and $\mathbf{f}$ is the external force per unit mass on each of the SPH particles. A suitable time step for the scheme therefore has the form

$$\Delta t = \frac{1}{4}\min\left(\Delta t_{cv}, \Delta t_f\right) \tag{51}$$

The coefficient in equation (51) can be increased slightly whilst still maintaining stability and various possibilities are suggested in the literature [23, 62].

Because of the way in which the symmetrical nature of the particle-particle interactions were maintained in the derivation of the basic SPH equations it is possible to ensure exact linear and angular momentum conservation if either a predictor-corrector or leapfrog method is used when solving the equations. Monaghan has also noted [53] that, with a correctly chosen time step, total energy is conserved to within 0.5% over 400 time steps. Both integration methods are second order accurate in time although only one force evaluation per time step is required.

2.8 Variable smoothing length

The smoothing length h represents the effective width of the kernel and its value determines the number of particles with which a given particle interacts. The accuracy of an SPH simulation depends on having a sufficient number of particles within the smoothing length to ensure that the replacement of an integral by a summation is valid. The speed of the computation however decreases as the number of such particles increases. The optimum number of particles has been discussed by Morris [61] and depends on the number of dimensions in the problem. In one, two and three-dimensional problems these are approximately 5, 21 and 57 respectively. These numbers are based on the number of neighbours on a cubic lattice with a smoothing length of 1.2 times the particle spacing and a kernel which extends out to $2h$.

If the fluid being modelled does not undergo substantial compression or refraction then a constant value for h is sufficient. However, if the density changes substantially during the course of a computation then h should be changed accordingly to maintain sufficient resolution. In the original formulations the resolution was constant in space but allowed to evolve in time, $h = h(t)$. A method to allow spatially varying resolution was introduced by Benz [3] and this resulted in enhanced accuracy and speed. In such schemes each particle has its own h depending on the local density in the particle's neighbourhood and the rate of change of the particle's density. For the simulation of incompressible fluids such as water for example, which are the main interest of this report, the density changes are restricted to be of the order of 1% and so a constant value of h was used in all the simulations described in the next section.

2.9 SPH coding details

There are a number of sites on the internet which provide access to free SPH codes. These include Joe Monaghan's home page at Monash University[1], which includes a number of sample FORTRAN codes for the simulation of both astrophysical and fluid dynamics problems, as well as a site at the National University of Singapore[2], which contains a FORTRAN code which was used to perform many of the simulation results discussed in the book by Liu and Liu [43].

Any SPH code basically solves a many-body problem in which, in principle, every particle interacts with every other particle in the problem. In practice, by using a kernel with compact support, such as that described by equation (11), each particle interacts with only a relatively small number of neighbouring particles confined within a radius of $2h$. Finding the nearest neighbours of any given particle is a major part of any SPH code. The simplest method of doing this is to calculate, for a given particle i, the distance r_{ij} from i to each particle j, where j = 1,2, …, N. If the distance r_{ij} is smaller than $2h$ then particle j is one of the nearest neighbours of particle i. The problem with this very simple all-pair search approach is that the time taken to perform this search is of order N^2, and for problems with more than a few thousand particles the computational time taken is simply too excessive.

Most SPH codes overcome this problem using either a tree search algorithm or a linked list algorithm. The tree search algorithm is popular in astrophysical SPH codes, particularly those including the effects of self-gravity, and works particularly well in problems in which h varies either in space or time. This reduces the computational time to $O(N \log N)$. The linked list algorithm works well for simulations in which h is spatially constant. Monaghan [53] has described the procedure for carrying out a nearest neighbour particle search using linked lists in the context of an SPH code. More details can be found in the paper by Riffert et al. [70] and the book by Hockney and Eastwood [30]. In essence, an auxiliary spatial grid is used to sort the particles into cells and then restrict the search to neighbouring cells. For example, if the kernel has compact support of length $2h$ then the mesh spacing should be set to $2h$. Then for a given particle i the nearest neighbouring particles can only be in the same grid cell or the immediately adjoining cells. Hence, in three dimensions, the search is confined to a maximum of 27 cells. The linked list algorithm allows each particle to be assigned to a cell and then all the particles in a given cell are linked together for easy access. The computational cost of this algorithm is approximately $O(N \times N_{neigh})$, where N_{neigh} is the average number of contributing neighbours per particle.

Another technique used in SPH codes to reduce the computational time is to use the symmetry (or antisymmetry) inherent in the particle-particle interactions. Given that the force on particle a due to particle b is equal in magnitude (but opposite in direction) to the force on particle b due to particle a, the time to perform summations such as those shown in equation (18) can be halved. The technique is to change the range of the indices in nested DO loops. The symmetry of the interactions allows nested loops where both a and b

---

[1] http://www.maths.monash.edu.au/~jjm/Teaching/welcome.html
[2] http://www.nus.edu.sg/ACES/software/SPH%20code/sph_code_in_the_sph_book.htm

go from 1 to N to be replaced by summations where a goes from 1 to N while b goes from a + 1 to N. Additional computational time can be saved by calculating the value of the kernel and its derivate over an appropriate spatial range at the start of the computation and then storing the values in a look-up table.

3. Illustrative examples for fluid simulations

In this section we illustrate the basic SPH formulation outlined above by applying it to some two-dimensional problems of interest to Maritime Platforms Division. The simulations were performed using software obtained from Joe Monaghan's website at Monash University and modified slightly by ourselves. All simulations were performed on a Pentium IV processor with 640 MB RAM running at 1.80 GHz. All programs are written in Fortran and a Compaq Visual Fortran 6 compiler was used to run the software. Typical run-times were no more than 30 minutes using up to 20,000 particles.

3.1 Classical dam break

Monaghan [54] used a simplified bursting dam problem as one of several examples to illustrate the ability of SPH to accurately model free surface flows. He performed two-dimensional simulations of the collapse of a liquid column and compared the results with the experiments of Martin and Moyce [46]. Both the height of the dam and the length of the surge front as a function of time were found to agree well with experiment, although the simulated position of the surge front was found to be slightly ahead of the experimental results in all the simulations. Monaghan attributed this to the effect of drag between the fluid and the bottom boundary particles. The boundary was simulated using a line of boundary particles and the force between the boundary particles and the fluid particles had the Lennard-Jones form given by equation (35). Monaghan noted that when the Lennard-Jones force was replaced by a gaussian force similar results were obtained.

Doring et al. [16] used both SPH and the Volume of Fluid (VOF) method of Nichols and Hirt [63] to simulate the experiments of Martin and Moyce [46] and found similar results; both the SPH and VOF simulations accurately reproduced the height of the dam as a function of time but the surge front was again slightly ahead of the experimental results. They suggested that this difference was probably due to the wall slip condition used in the calculations. Colagrossi and Landrini [11] used SPH, a boundary-element method, and a Level Set method to simulate the same experiments and again found similar results; all the numerical solutions agreed very well, but the surge front was again slightly ahead of the experimental results. They attributed the disagreement to experimental uncertainties in the early part of the experiment and to the neglect of important physical effects on the longer time scale. They suggested that an important effect which was not included in their modelling was the bottom-induced drag which altered the propagation velocity and triggered the development of turbulence near the water front. Liu and Liu [43] also simulated these experiments using the SPH code described in their book and obtained results which are more accurate than those calculated by Monaghan [54].
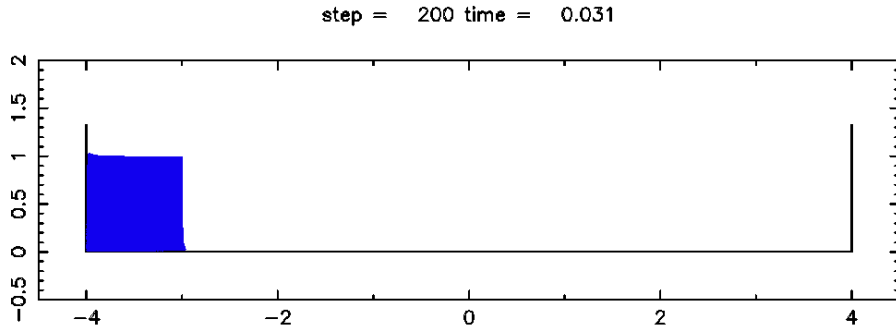
step =   200 time =   0.031

Figure 1:   Particle configuration for the collapsing water column at t = 0.031 α = 0.001 and total number of particles = 15,440. Lengths are measured in metres

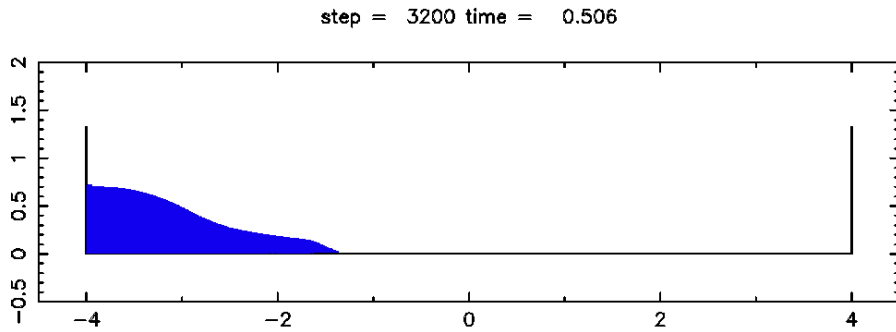step =   3200 time =   0.506

Figure 2:   Particle configuration for the collapsing water column at t = 0.506 α = 0.001 and total number of particles = 15,440. Lengths are measured in metres
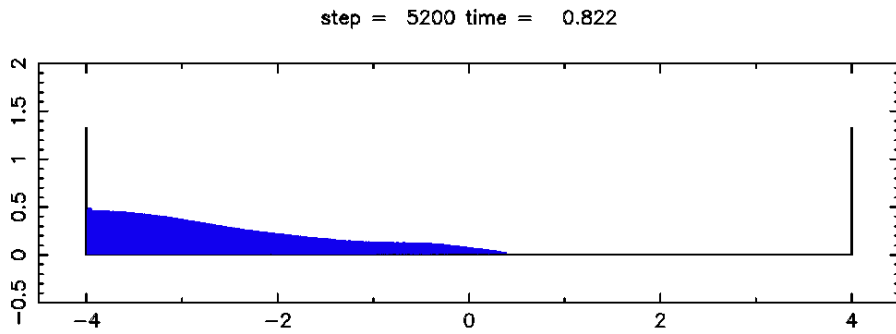
step =   5200 time =   0.822

Figure 3:   Particle configuration for the collapsing water column at t = 0.822 α = 0.001 and total number of particles = 15,440. Lengths are measured in metres

They claim that this is due to their use of type II boundary virtual particles in addition to the type I boundary particles used by Monaghan; their use of these additional virtual boundary particles in the summation process increases the drag force for the particles near the bottom.

We have simulated the experiments of Martin and Moyce [46] using a two-dimensional implementation of the SPH formulation outlined in Section 2. Figures 1, 2 and 3 show the particle configuration for the collapsing water column at representative times. Boundary particles were used to form the left-hand boundary, the base, and the right-hand boundary. Three different types of boundary force expressions were tried. Each of these had the form given by equation (36) in Section 2.6 with the function P(x) given by equation (39). The function R(y) had three different forms, depending on the parameter *potsw*. If *potsw* = 1 then R(y) is an integral repulsive force having the form given by equation (37). If *potsw* = 2 then R(y) is logarithmically singular and has the functional form A($1/q$ – 1). If *potsw* = 3 then R(y) is based on the derivative of the kernel and has the form given by equation (40).

The particles are initially set up on a cartesian lattice and the smoothing length is defined as $h = 1.2 \, \Delta p$, where Δp is the initial particle spacing. In all the simulations described here h is constant in space and time and has the same value for each particle. Due to the manner in which the particles are initially placed in the domain the system is not in equilibrium at t = 0 and so a damping force is applied to the particles for the first few hundred time steps. This has the effect of settling the system down to an equilibrium state and is an important part of the calculation.

Figures 4 and 5 show the simulated height and surge front position as a function of time. All lengths are scaled by the initial height of the water column (H0) and time is scaled by the factor $(H_0/g)^{1/2}$. Three different runs are shown, corresponding to *potsw* = 1, 2 and 3. In each run α = 0.001 and the total number of particles was 15,440. Figure 4 shows excellent agreement between the experimental results and the simulated results for the height of the water column as a function of time. In Figure 5 the agreement with experiment is excellent for early times, but the simulated surge front position leads the experimental values at later times. This behaviour is the same as that found by Monaghan [54], Doring et al. [16], and Colagrossi and Landrini [11] and is caused by the lack of rigour in the specification of the exact boundary condition at the water/boundary interface. The effect is most pronounced at the tip of the surge front because the water layer is very thin at this location and the boundary forces provide the controlling influence. Both Figures 4 and 5 show that the assumed form of the boundary force has negligible effect on the accuracy of the simulated results.
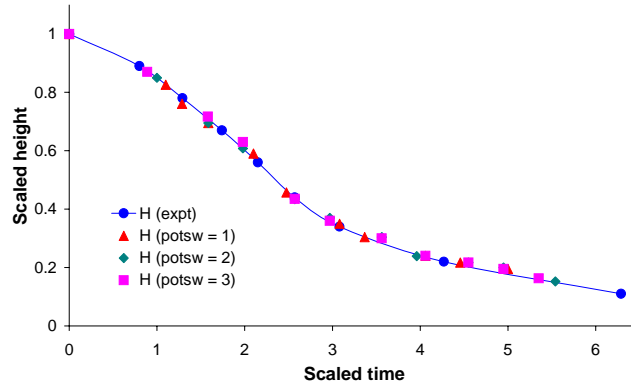
Figure 4:   Height of water column as a function of time. α = 0.001 and the number of particles = 15,440
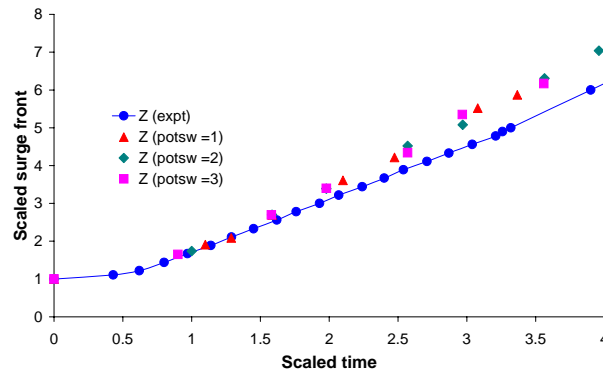

Figure 5:   Position of surge front as a function of time. α = 0.001 and the total number of particles = 15,440

Figure 6 shows the effect of changing both the resolution of the calculation and the assumed value of α on the height of the water column as a function of time. In the figures *ny* represents the number of water particles initially placed next to the left hand boundary of the container. For *ny* = 80, 120 and 160 the total number of particles in the calculation is 7,120, 15,440 and 26,960 respectively and the corresponding value of *h* is 1.5 cm, 1.0 cm and 0.75 cm. As can be seen, the simulated results are virtually independent of the resolution for the range considered here. Also, changing α between α = 0.001 and α = 0.01 has little effect on the calculated values. Similar conclusions can be drawn from Figure 7, which shows the effect of the above changes in computational parameters on the simulated surge front position as a function of time.
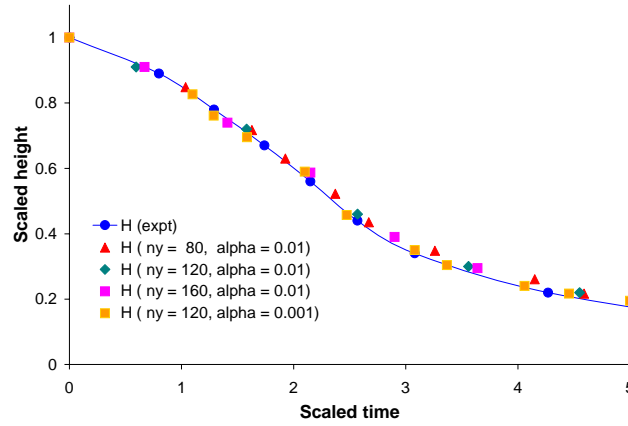
Figure 6: Height of water column as a function of time. $\alpha = 0.01$ and the number of particles varies between 7,120 and 26,960
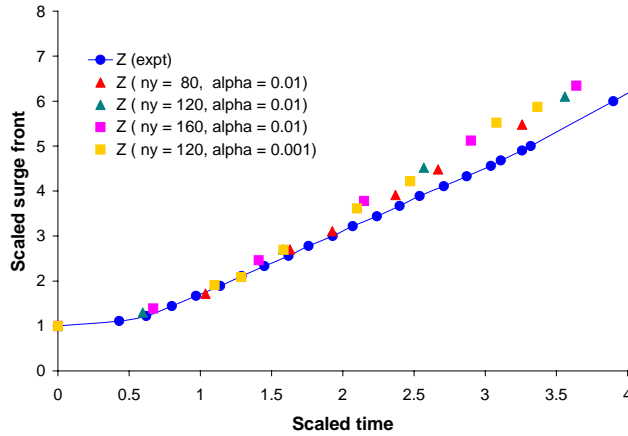

Figure 7: Position of surge front as a function of time. $\alpha = 0.01$ and the total number of particles varies between 7,120 and 26,960

3.2 Sloshing

Sloshing is defined as the relative motion of a fluid with a free surface confined inside a tank caused by the motion of the tank itself. It is a highly non-linear resonant phenomenon appearing in all marine structures containing liquids and is of critical concern in the design process because its occurrence can lead to excessively high dynamic loads on the tank walls. The simplest method to simulate the effects of sloshing is to use an analogy with a coupled mass and spring system, but this does not allow the pressure on the container wall to be calculated. Solaas and Faltinsen [71] analysed the sloshing problem using the potential flow hypothesis by decomposing the free surface into a sum of periodic modes. This method works well if the deformations of the free surface are not extreme, but is unable to cope with events such as wave breaking and roof impacts, both of which are common phenomenon in ship tanks.

The availability of commercial finite element and finite volume software packages such as LS-DYNA, FIDAP, Fluent and CFX over the past twenty years provides a more accurate method of simulating sloshing phenomena. Tracking the free-surface of the fluid over the computational mesh is still a difficult problem however and some of the methods which have been created to overcome this problem include the Marker and Cell (MAC) method of Harlow and Welsh [28], the Level Set technique of Osher and Sethian [67] and the Volume of Fluid (VOF) method due to Nichols and Hirt [63]. Whilst each of these methods works well in particular situations they are computationally involved and expensive. SPH offers a much more natural way of dealing with free-surface problems and it is natural to turn to this method when attempting to simulate sloshing phenomena.

Delorme et al. [14] used a two-dimensional SPH method to calculate the sloshing pressure for LNG tankers and found good agreement with results calculated using a MAC code. Souto Iglesias et al. [72] have used SPH to simulate sloshing in passive roll-damper tanks for fishing vessels. They compared their results against experimental data and found good agreement, both for quantitative physical magnitudes such as moment phase lags, as well as more qualitative ones such as free surface shapes. Doring et al. [16] have performed two-dimensional SPH simulations of sloshing in a test tank and compared the computed free surface shapes with the experiments of Corrignan [13]. Excellent agreement is obtained between the simulated and experimental surface profiles, even though considerable non-linearity is observed.

In this section we have modified the SPH code described in Section 2 and used in Section 3.1 to simulate the dam breaking problem by allowing the boundary particles which form the liquid container to oscillate horizontally. This allows us to simulate the free surface shapes obtained in the experiments of Corrignan [13]. In these experiments a rectangular tank 40 cm wide and 20 cm high containing water to a height of 12 cm is forced to oscillate horizontally with a time dependence given by

$$x(t) = A_0 \left[\sin(2\pi f_1 t) - \sin(2\pi f_2 t) \right] \tag{52}$$

where $A_0 = 0.75$ cm, $f_1 = 1.598$ Hz and $f_2 = 1.307$ Hz. The only changes to the code required to do this are to prescribe the motion of the boundary particles in both the predictor and corrector parts of the time integration routine. Initially we forced both the position and velocity of these particles according to equation (52), but found that this lead to instabilities in the code and resulted in some particles being forcefully ejected from the fluid domain. Stable behaviour was obtained by specifying the velocity only, and then calculating the position from the equation

$$r_a = r_a^0 + \Delta t \, v_a^0 \tag{53}$$

Equation (53) was only applied during the predictor step, whilst the velocity was prescribed during both the predictor and corrector step. This small change in the computational procedure lead to remarkably stable behaviour and the code was well behaved over many tens of thousands of time steps. We are uncertain as to why this particular procedure works as well as it does, although we note that it is similar to the type of instability which occurs in many CFD codes when certain boundary conditions are over prescribed.

It is interesting to note that Gomez-Gesteira et al. [26] found similar behaviour in their two-dimensional SPH code. They used SPH to model wave overtopping on the decks of offshore platforms and ships and used moving boundary particles to create the initial waves. They externally imposed both position and velocity on the boundary particles and found that this gave rise to instabilities and very high instantaneous accelerations and forces. They solved this problem by imposing a smoothing function on both the prescribed position and velocity.

Figures 8 and 9 show computed free surface shapes at selected times for a calculation using 15,440 particles. Figure 10 shows the comparison between the computed surface shapes and the experimentally measured profiles. The agreement is remarkably good, especially considering the relative simplicity of the code employed. A similar calculation using either a finite difference, finite volume or finite element code would involve far more computational complexity and hence significantly increased computational time. The increased computational effort when using a grid-based code results from both the need to use specialised algorithms to locate or track the interface, as well as the extra coding involved to keep track of the moving mesh. The amount of coding required to implement either of these features in a grid-based code is often greater than that used to solve the basic fluid equations. In an SPH simulation, however, no extra coding is required to locate the interface and in the two-dimensional calculation shown here only a few extra lines of coding were needed to effectively simulate the moving boundaries.

The accuracy of the comparison between the computed and experimental surface shapes shown in Figure 10 is typical of the accuracy of SPH simulations. Other examples of this type of simulation are easily found. Next Limit Technologies provide several examples on their website[3]. These simulations are conducted using their particle simulation code called XFLOW, which is based on the SPH method, and show two-dimensional simulations of sloshing flow and comparisons with the experimental results by overlaying the simulated results on the real video footage of the experiment. The simulations run for extended periods of time and show no degradation in the accuracy of the simulated surface shapes as the length of the simulation time increases.

3.3 Wave breaking over ships

Water impact loading on offshore structures is a subject area which is now becoming amenable to detailed study using sophisticated computational fluid dynamics codes. Both Neilson [64] and Kleefsen [38] have recently studied the green water problem, where large masses of water can invade a ship's deck in rough seas and cause considerable damage to the ship, or to equipment or personnel on the deck. Both these authors used finite volume CFD codes and variations of the VOF method to capture the free surface motion of the breaking waves and obtained good agreement with experimental results, where available for comparison.
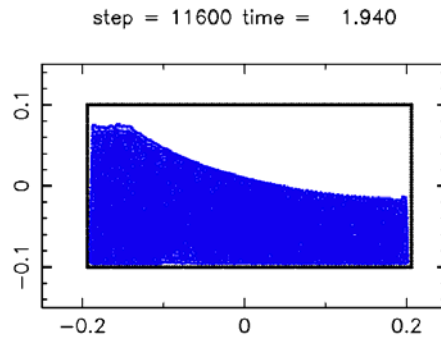
---

[3] http://www.nextlimit.com/xflow/index.htm

Figure 8:   Simulated free surface shape for sloshing tank at t = 1.94 seconds. Lengths are measured in metres
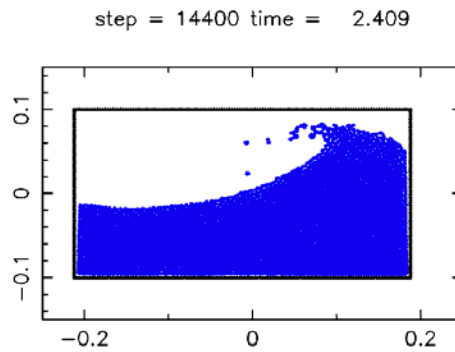

Figure 9:   Simulated free surface shape for sloshing tank at t = 2.409 seconds. Lengths are measured in metres
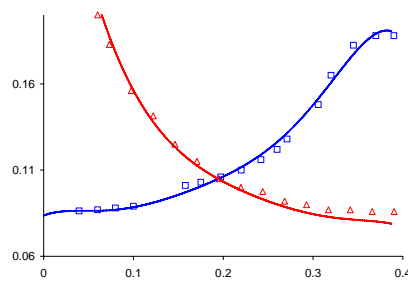

Figure 10: Comparison between computed and experimental surface shapes. Blue = 1.65 seconds, red = 2.0 seconds. The solid curves are the SPH results while the symbols represent the experimental results

The use of an Eulerian grid to model both the bulk of the sea water and the ship itself however inevitably results in restrictions on the amount of the ship structure which can be included in the simulation. The success of SPH demonstrated so far in accurately simulating free surface motion naturally leads to the idea of combining SPH to model the fluid motion with either a finite volume or finite element code to model the ship structure. A number of authors have already addressed this problem and encouraging results are being obtained. Gomez-Gestiera et al. [26] have used SPH to simulate a simplified model of the green water problem. They found that the wave profiles generated by the method were in good quantitative agreement with the experimental ones and that the simulation successfully reproduced the main features observed when a wave hits a horizontal platform. Gomez-Gesteira and Dalrymple [25] have used a three-dimensional SPH code to model wave impact on a tall structure and found that the velocities and forces obtained from their numerical code were in excellent agreement with model laboratory measurements. Fontaine [19] has also used SPH to model extreme waves and their interaction with a structure and Oger et al. [65] have used SPH to simulate wave-body interactions in extreme seas. In this section we present a very simplified model of a ship sinking in rough seas to illustrate the capability of SPH to handle this scenario. The model is similar to one recently presented by Doring et al. [17]. It should be noted that the simulation shown here has been constructed to illustrate the capabilities of the SPH technique in a simplified situation; hence there is no experimental data for comparison.

Figure 11 shows a sequence in which our model ship (a rectangular box with a slit in the side to allow ingress of water) is initially placed above the surface of the water and then allowed to fall under gravity. The box then oscillates in a vertical plane until the buoyancy force balances the gravitational force and the box comes to a stable equilibrium floating on the water surface. At time t = 2.335 seconds the tank containing the water is oscillated horizontally to induce strong wave motion. Between t = 5.0 seconds and t = 5.4 seconds the action of the waves breaking over the box results in considerable ingress of water and the box eventually sinks to the bottom of the tank after 7 seconds.

The code used to perform this simulation was the same one which was used to calculate the results shown in sections 3.1 and 3.2. To perform the current simulation additional boundary particles were added to create the floating box. A subroutine was then written which took the total force on the box due to all the fluid particles and then moved the centre of mass of the box in accordance with this force. The boundary particles forming the box were then moved in relation to the centre of mass of the box to simulate the motion of a rigid body. The additional coding required to perform this simulation was again minimal, partly because we did not allow the box to rotate about its centre of mass. This would have involved some complicated geometry to calculate the new positions of the normals to the boundary particles and time constraints on the work did not allow this level of complexity. Nevertheless, this example clearly illustrates the ability of the SPH method to cope with quite complicated fluid-structure interactions using relatively simple coding. A comparable simulation using a grid-based code would involve an order of magnitude increase in the level of complexity of the coding and the simulation time, for reasons similar to those mentioned in the previous section. As well as the need to use specialised algorithms to locate the interface and move the mesh additional coding is also required for the fluid-body interaction.
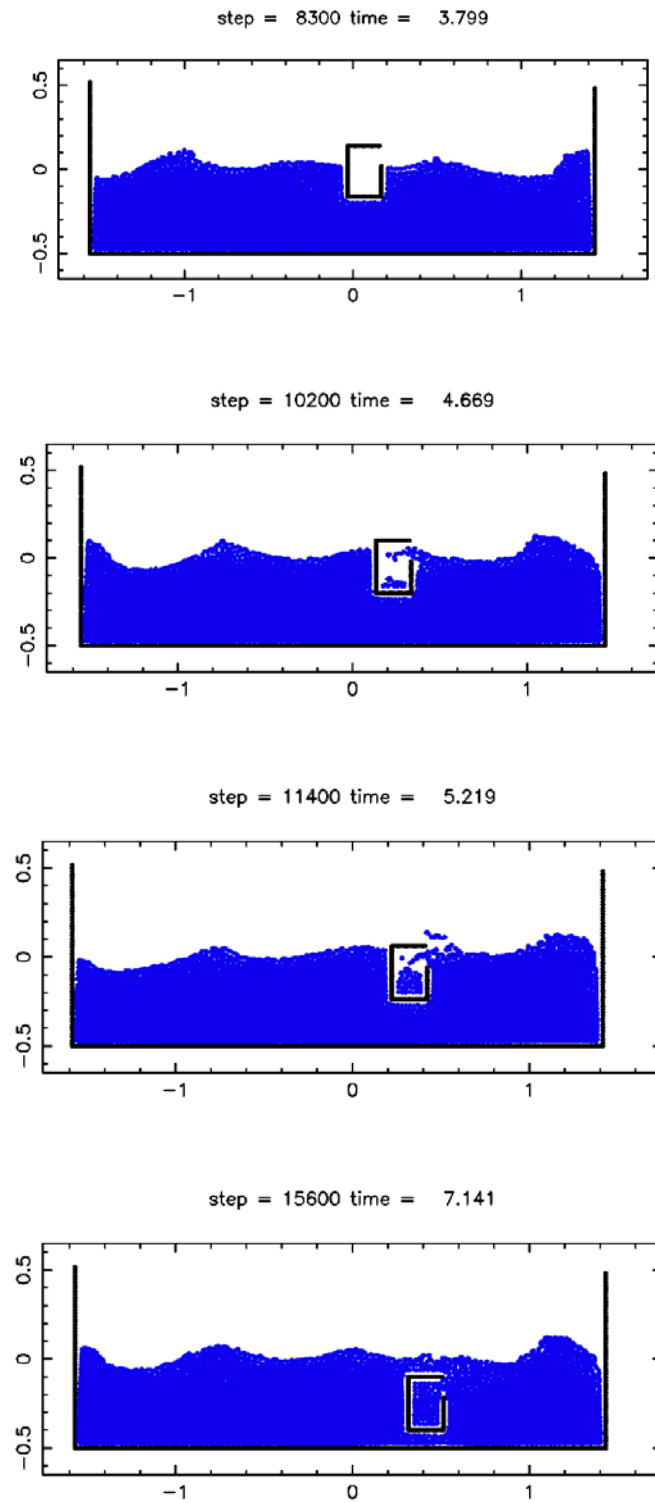
Figure 11: Sequence showing the sinking of an empty container due to ingress of water via wave motion. Lengths are measured in metres

May and Monaghan [47] have recently performed a similar two-dimensional SPH calculation to investigate the possibility that a large bubble of methane gas released by the ocean floor could capsize a floating body. In their simulation the model ship was also constructed from additional SPH boundary particles and was allowed to rotate as well as move in the horizontal and vertical directions. Their simulations showed that when the radius of the bubble is comparable to the length of the ship's hull that it is possible for the bubble to cause the ship to sink. This is due to the mound of water which is raised above the rising bubble and the subsequent flow of water from the mound which creates a deep trough either side of the mound, which can then carry the boat into the trough.

A more sophisticated approach to the sinking of ships due to either rough seas or bubble dynamics produced by underwater explosions or natural methane gas eruptions would be to couple the SPH code to a fully fledged finite element code. Considerable progress along these lines has already been made by Cartwright et al. [5], [6] and [7]. These authors have used an SPH model embedded in the commercial finite element code PAM-SHOCK to simulate the non-steady motion of various vessels in varying sea conditions. The simulations to date have used rigid finite element models for the vessels so that accurate force magnitudes could not be obtained. Nevertheless, the simulated vessel motion displays qualitatively correct behaviour for all of the vessels studied. A simulation of the Incat 91 metre Wave Piercing Catamaran showed that dynamic lift from the under body shape of the hull was developed as the correct cruise speed was approached [5], while in a further application the method was shown to account for the correct dynamic loads on a 34 metre catamaran sailing yacht [6]. The most advanced application of this method to date has been to the simulation of the motion of a landing craft within the flooded well dock of a parent ship [7]. Very encouraging preliminary results have been obtained and this example will be discussed in more detail in Section 5.

4. Applications to solid mechanics modelling

Problems involving large scale material deformation have always been of interest to the defence community. Examples include deformation due to high-velocity impact, the fracture and fragmentation of cased explosives, the formation and penetration of shaped charge jets, and debris cloud dynamics due to hypervelocity impact. The simulation of these problems has traditionally been conducted using large computer programs known as hydrocodes, which solve the continuum equations for the conservation of mass, momentum and energy in combination with sophisticated equations of state which describe material behaviour.

During the 1980s and 1990s WSD used a number of these codes to assist in the design of various warheads and the analysis of their behaviour. The Lagrangian finite element code DYNA2D was used to model the formation of Explosively Formed Projectiles (EFPs) [32], Shaped Charge jets [33], the investigation of limpet mine damage effects against ship hulls [75], and the design of an EFP to be used as a stand-off sea mine neutralisation device [40]. The use of Lagrangian codes to simulate material response is limited to cases where the amount of deformation is small. When the deformation is large, Eulerian codes must be used and WSD used the finite volume Eulerian codes HELP [27] and HULL [18] in these situations. These codes can handle arbitrarily large material deformations but require

sophisticated coding techniques to model material interfaces. Difficulties can also occur when simulating problems with fracture, void formation, and fragmentation.

During the period 1990-1996 defence scientists in both the USA and UK became aware of the unique capabilities of the SPH method and began to adapt it to the solution of solid mechanics problems relevant to the defence community. Although the name Smoothed Particle Hydrodynamics might be thought to imply that only hydrodynamic problems could be addressed by the method, material strength can in fact be added in a fairly straight forward manner. Libersky and Petschek [41] were the first to show how this could be done by incorporating an elastic-perfectly-plastic material strength model into the SPH framework and applying it to the simulation of the impact of an iron rod with a rigid surface. Early results were quite encouraging and the method was quickly extended into the three-dimensional shock and material response code MAGI [42], which was based entirely on the SPH method. The code was used to model additional cylinder impact tests and the debris cloud resulting from the hypervelocity impact of a copper disc on an aluminium plate. A companion paper using two-dimensional calculations [68] (therefore achieving a significantly finer resolution) of the same hypervelocity impact problem showed superb agreement between the SPH particle plot and the X-ray photographs of the debris cloud.

An excellent summary of the early work of Libersky, Petschek and co-workers can be found in the paper by Randles and Libersky [69]. This paper also highlights the significant advantages of the SPH method for simulating the dynamic response of materials involving fracture and fragmentation. Several simulations of the detonation of cased explosives are given, including a simulation of the detonation of a MK82 general purpose bomb out to 280 μs. The fragment distribution data was found to compare remarkably well with the experimental data.

It should be stressed that a very important property of the SPH method is that it allows a totally seamless transition between a fully continuum description of matter and the transformation of the material into any number of fragments produced by impact. At least one noted authority in this area believes that it is definitely the best method for dealing with the fragmentation of brittle solids by impact [56]. The only underlying problem with the application of SPH in this area is that the normal SPH elastic equations do not conserve angular momentum. This has been noted by Monaghan [56] and discussed by Hoover et al. [31], who have shown that by using strong XSPH smoothing the loss in angular momentum of a rotating elastic wheel can be considerably reduced.

A more common approach to the use of SPH methods in the simulation of problems involving large scale material deformation and fracture is to couple the SPH method with a standard Lagrangian finite element code. The Lagrange method (where the mesh distorts with the material) has the advantage of being fast and providing excellent definition of the material interfaces. When the deformation becomes too large however the grid becomes entangled and the calculation stops. Lagrangian codes try to overcome this problem by using an erosion algorithm, where elements which have reached a specified value of strain (typically 150%) are simply removed from the grid. This is obviously a non-physical process however and results in energy being artificially removed from the calculation.

SPH provides the perfect solution to this problem; as the elements become highly strained they are simply converted to SPH nodes. This immediately removes the problem of grid

entanglement as the SPH particles are never required to have any connectivity. Johnson et al. [34] were the first to show how this could be achieved using the Lagrangian finite element code EPIC. A two-dimensional axisymmetric version of the code was used and simulation results were shown for both cylinder impact and hypervelocity impacts with a variety of different material models including copper, iron, steel, aluminium and concrete. Comparison with experimental results was excellent. More details of the method, and more simulation results for high velocity impact problems, are provided in Johnson [35] and Johnson et al. [36].

Shortly after the work of Johnson appeared Swegle and Attaway [73] coupled the SPH method into the transient dynamics finite element code PRONTO and used it to simulate a number of underwater explosion problems involving fluid-structure and shock-structure interactions. Their results showed that this combined method was well-suited to model the transmission of loads from underwater explosions to nearby structures. Bubble formation and collapse was also modelled effectively, although the authors noted that the method still had difficulty (like all previous methods) in calculating the late time effects due to the acceleration of gravity and bubble buoyancy.

Following on from the work of Johnson et al. [34] and Swegle and Attaway [73], Hayhurst et al. [29] implemented an SPH module in the two-dimensional axisymmetric version of the AUTODYN hydrocode for the simulation of ballistic impact problems. AUTODYN is a fully integrated suite of codes incorporating Lagrange, Shell, ALE (Arbitrary Lagrange Eulerian) and Eulerian solution techniques which can be coupled in several ways in space and time. Previous numerical simulations of ballistic impact problems using AUTODYN used either the Lagrange or Euler processors, both of which have significant failings in certain areas. As noted, the Lagrangian method suffers from grid entanglement problems when the material deformation becomes large. This problem can be overcome using the Eulerian approach, where the grid remains fixed in space, but the codes are considerably more expensive to run due to the complicated algorithms required to resolve material interfaces, and the method is also ill-suited to the implementation of sophisticated fracture mechanics models, which require the complete history of the material to be followed (which is the case with the Lagrangian approach).

Hayhurst et al. [29] tested their SPH version of AUTODYN-2D by simulating the impact of an iron cylinder on a rigid wall, a steel projectile impacting a ceramic target backed by aluminium, and the penetration of a tungsten long rod into a thick steel target. In each case the SPH simulation performed as well or better than simulations using either the Euler or Lagrange processors. They concluded by noting that the combination of an SPH algorithm with a Lagrangian processor maintained all the advantages of the Lagrangian method, such as the efficient tracking of material interfaces and the ability to incorporate sophisticated material models, while removing the problem of grid tangling in a physically realistic manner.

Clegg et al. [10] further pursued this approach by using the SPH capability in AUTODYN-2D to simulate kinetic energy penetrator impacts on multi-layered soil and concrete targets. The advantages of the technique were clearly highlighted in this series of simulations because the extent of cracking in the concrete was far more realistically simulated using the combined Lagrangian/SPH method. Neither the Eulerian nor Lagrangian calculations were as effective in predicting spall from both the front and back

sides of the target. The use of the Lagrangian/SPH technique allowed sophisticated constitutive models to describe the concrete behaviour, such as hydrostatic compaction, yielding, damage and cracking, which are extremely difficult to implement in Eulerian codes, while overcoming the problem of mesh tangling. The method proved to be so successful that the SPH method was implemented in AUTODYN-3D and was used to simulate the formation of an Explosively Formed Penetrator (EFP), a Shaped Charge Jet, and hard penetrator impact onto ceramic armour [66]. This version of the code has also been used to model the impact of stainless steel and tantalum projectiles onto transparent targets at speeds which are sufficiently high enough to result in the shattering of the projectile.

In the discussion regarding wave breaking over ships in Section 3.3 it was noted that the finite element code PAM-SHOCK contained an SPH module and that the code had been used to simulate the non-steady motion of vessels in varying sea conditions. In that application of the code the SPH module was used to model the bulk motion of the water. Kamoulakos et al. [37] have used the SPH module in PAM-SHOCK for a completely different application. They conducted a number of space debris impact simulations on Whipple shields using both the SPH option and the finite element version of the code and found good agreement with experiment using both methods.

The Livermore Software Technology Corporation software LS-DYNA is another example of a commercial finite element code which has recently been coupled with an SPH module. Details of the implementation can by found in the paper by Lacome [39], which also contains examples of the application of the combined finite element/SPH solver to the simulation of bird impacts on turbine blades and various types of ballistic impact.

De Vuyst et al. [15] have recently implemented an SPH algorithm in the public domain version of the DYNA code. Their method of implementation uses a contact force vector to treat the finite element nodes as SPH particles. This is different to the earlier implementations of SPH in finite element codes, which typically used a master-slave algorithm to couple the two techniques. The performance of their algorithm is illustrated by the simulation of three diverse impact problems: a plate impact, water impact and rod penetration. Excellent agreement was found between the simulation results and the experimental or numerical results for each of these problems.

5. Current SPH work in MPD

Several research groups within MPD are currently using, or planning to use, the SPH technique for the simulation of a number of different problems. These include the relative motion of a landing craft and the mother ship in a well dock scenario, sloshing within hulls, underwater explosion events, the deployment and retrieval of autonomous vehicles, and ballistic impact on ceramic targets. This section briefly describes each of these areas of application.

5.1 Surface Platform Systems Branch

The examples described in Section 3 of this report show that SPH provides a convenient, simple and robust method for the study of free surface fluid motion. It is this aspect of

SPH which makes it a particularly useful tool with several areas of application within the Surface Platform Systems (SPS) Branch.

One of the current major projects for the ADO is the acquisition of two large amphibious Landing Helicopter Dock (LHD) ships containing well docks. In order for DSTO to be able to provide advice to minimise the risk associated with potential operational constraints during the selection of the final design there is a need to be able to simulate the relative motion between the LHD and the landing craft within the well dock. Using conventional finite element, finite difference or finite volume codes this would be a problem of considerable difficulty and limited application. The combination of a finite element code to model the LHD and the landing craft with an SPH module to model the fluid motion however makes this problem much more amenable to simulation.

Considerable progress in this area has already been made by Cartwright and McGuckin of Pacific ESI in collaboration with Stuart Cannon and Terry Turner from the SPS branch. They used the Pacific ESI finite element code PAM-SHOCK, which contains an embedded SPH module, to simulate the motion of two generic landing craft models within the well dock of a parent ship [6]. Figure 12, an illustration of the capability of the code, shows a landing craft about to enter the flooded well dock of a parent ship.

Simulations were run for two scenarios. In the first the landing craft was tethered in a fixed position, while in the second the landing craft was moving forward within the well dock. The results showed that this method provided a viable simulation tool for the prediction of the relative motion between the LHD and the landing craft, although it was noted that several research challenges needed to be solved and experimental validation was required before the method could be considered ready for application to a specific problem.

One of the problems with the SPH method, noted by Cartwright et al. in a previous paper [6], is that considerable loss of wave amplitude can occur in an SPH simulation if a wave is propagated over distances of more than several wavelengths. This problem is currently being addressed by Cannon and Turner in collaboration with Joe Monaghan (Monash University) and Paul Cleary (CSIRO). Experimental wave data obtained by Turner in the towing tank at the Australian Maritime College in Launceston is being used to benchmark simulations conducted by Monaghan and Cleary using in-house SPH codes. Once the cause of the energy loss is identified and appropriate solution strategies are implemented it is anticipated that these refined SPH methods will be implemented in future SPH-finite element code combinations and lead to more accurate predictive capabilities. Current work in this area recently reported by Monaghan [56] has shown that by using a different time stepping algorithm there was little decrease in amplitude over five wavelengths, but that wave heights had reduced to about 60% of the initial amplitude after propagating over ten wavelengths. This problem does not occur with the simulation of solitary waves generated by a numerical wavemaker.
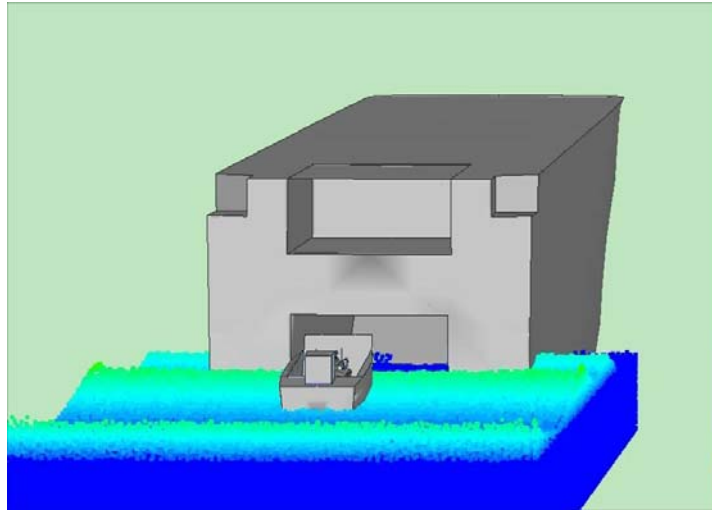
Figure 12: Simulation of the docking of a landing craft within an LHD ship using the PAM-SHOCK finite-element/SPH software

Another problem of current interest within the SPS branch concerns sloshing within ship hulls. Interest in this area has been stimulated by the recent grounding of HMS Nottingham on Wolfe Rock near Norfolk Island. The ingress of water and the internal sloshing caused by the motion of the grounded ship due to the impact of the waves lead to significant weakening of the internal bulkheads. Initial simulation work in this area is currently being done using the LS-DYNA finite element code, which also contains a coupled SPH module for the simulation of fluid motion. As a precursor to the simulation of a complete hull DYNA is currently being used to simulate the sloshing experiments of Neilson [64]. Results to date show that the code can accurately calculate the shape of the fluid surface, but some problems are being experienced in calculating accurate pressure loadings on the tank walls.

This is not an uncommon situation with current SPH calculations. The method works remarkably well in areas remote from boundaries, but special effort is required to accurately represent forces on boundaries. As mentioned in Section 3.3, Gomez-Gesteira and Dalrymple [25] have used a three-dimensional SPH code to model wave impact on a tall structure and found that pressure loadings obtained from their numerical code were in excellent agreement with model laboratory measurements. They achieved this result by treating the boundary particles as fixed fluid particles. The advantage of this approach is that it is unnecessary to make an *a priori* assumption about the nature of the force exerted by the boundaries, nor to utilize special computations there; a repulsive force normal to the boundary results without any additional considerations.

Once the boundary force problems in DYNA have been overcome it is anticipated that the code will then be used to simulate loads on ship bulkheads. This information will then be used as input to short term damage assessment codes currently in use in MPD. This will give an assessment of the strength of the vessel in such situations and aid in the initial application of damage control procedures.

As mentioned in Section 4.0, SPH has already been applied to the simulation of underwater shock and bubble dynamics produced by the detonation of underwater explosives. An understanding of these events and an ability to predict their behaviour is vital for the prediction of warship survivability. DSTO has therefore been engaged in an experimental and computational study of underwater explosions for some years now, with the ultimate aim of developing a realistic simulation capability for their effects on naval vessels. To date this work has been carried out with both Lagrangian and Eulerian finite element codes. These mesh-based techniques have limited success in following the changing bubble geometry over the course of several bubble expansions and contractions however and so some preliminary work is being done on this problem using the SPH method. This is a collaborative project between Dr. Irene Penesis at the Australian Maritime College in Launceston and the group led by Dr. John Brett in MPD. Initial studies will be performed using the SPH code described in the book by Lui and Lui [43], suitably modified for the modelling of underwater explosives. The project will simulate the motion of explosive bubbles and compare the simulated results with experimental data obtained by the MPD group from experiments conducted in Epping quarry.

5.2 Undersea Platform Systems Branch

An ideal tool for maritime automation research has recently been developed in the UPS branch by John Wharington. The software is known as Odessa and provides an integrated simulation environment for vehicular and articulated systems. It simulates the motion of multiple rigid bodies interlinked by various types of joints and has applications in many maritime scenarios including simulation of AUV, ROV and UAV dynamics, payload drops, decoys and towed arrays. Odessa is based on ODE (Open Dynamics Engine), an open-source package used primarily for game development. The software uses the LCP (Linear Constraint Problem) formulation but makes various approximations in order to produce faster simulations with greater robustness.

Odessa incorporates a special cable modelling package developed at RMIT University over the past decade which is specific to DSTO requirements. This specialized cable code is faster and more accurate than using primitive elements and is capable of explicit incorporation of bending, torsional stiffness, and hydrodynamic loads, thus making it ideal for the simulation of umbilical cables on ROVs and AUVs, multipart tow systems, and towed arrays.

To extend the capabilities of Odessa to allow the code to model complex multibody interactions involving fluids, a new fluids simulation module has been written and integrated into the software by Royce Smart. Because the applications envisaged include highly non-linear free surface fluid motion the software uses the SPH method. The code is based on the SPH program contained in the book by Liu and Liu [43] but has been completely re-written in C++ to more easily interface with the Odessa code and the graphics software. The use of the SPH technique is also appropriate because the method is remarkably robust and can be adjusted to provide a trade off between speed and accuracy, which is also a feature of the underlying LCP method in Odessa.

The incorporation of the SPH module in Odessa will allow the code to model well-dock scenarios and the deployment and retrieval of autonomous vehicles. This work is complementary to the well-dock simulations conducted in the SPS branch conducted by

Cannon and Turner using PAM-SHOCK because the sophisticated cable model in Odessa will allow more realistic simulations of the various methods of restraining the landing craft within the well-dock, while the finite element capabilities in PAM-SHOCK will allows more realistic simulations of individual types of landing craft.

The current capability of the SPH module within Odessa is illustrated in Figure 13, which shows a sequence in the damn break problem at intervals of 0.5 seconds. The code is fully three-dimensional and the illustrations show an SPH fluid interacting with Odessa rigid body objects, which are the transparent walls of the container. The SPH particles are colour coded by velocity, with blue being the lowest velocity and red the highest velocity.

5.3 Advanced Materials and Sensors Branch

MPD has core responsibility for research into enhancing military vehicle survivability and has a long history of achievement in ballistic protection research in all areas of armour technology. Predictive modelling plays a significant role in evaluating the performance of various types of armour against ballistic impact and previous work in this area has been conducted using the Lagrangian finite element code DYNA.

The prevalence of new composite armours containing ceramic layers however has lead to a need to upgrade current simulation capabilities to deal with the complicated fracture mechanics of these types of materials. Stephen Cimpoeru and his team in the AM&S branch are planning to use the SPH module in the AUTODYN software package to simulate the ballistic protection offered by confined and unconfined ceramic targets and transparent armour. As discussed in Section 4.0, the SPH module within AUTODYN has already displayed considerable success in simulations of this type. The combination of the finite element Lagrangian solver with the SPH module and the sophisticated materials models within AUTODYN, which includes constitutive models for metals, composites, ceramics, glass, concrete, soil, and explosives, currently provides the most appropriate tools for modelling ballistic impact events of this type.

6. Discussion and Conclusion

The use of the SPH technique for the simulation of hydrodynamic flows, gas dynamics and solids modelling has increased significantly during the past decade. The areas in which SPH has found application are now so diverse that no review can authoritatively cover each of these areas in significant detail. The simulations and applications discussed in this report have concentrated on those areas thought to be of most use to current defence science interests.

A large body of work has now shown that SPH is a particularly useful tool for the prediction of bulk fluid motion with free surfaces. SPH is clearly the best numerical technique to apply to these types of problems if the simulated results for the fluid motion are not required to display extremely high levels of accuracy, which is typically the case in many defence applications. Examples of this type of application include the sloshing of water inside hulls, the well dock problem, and wave breaking over ships.
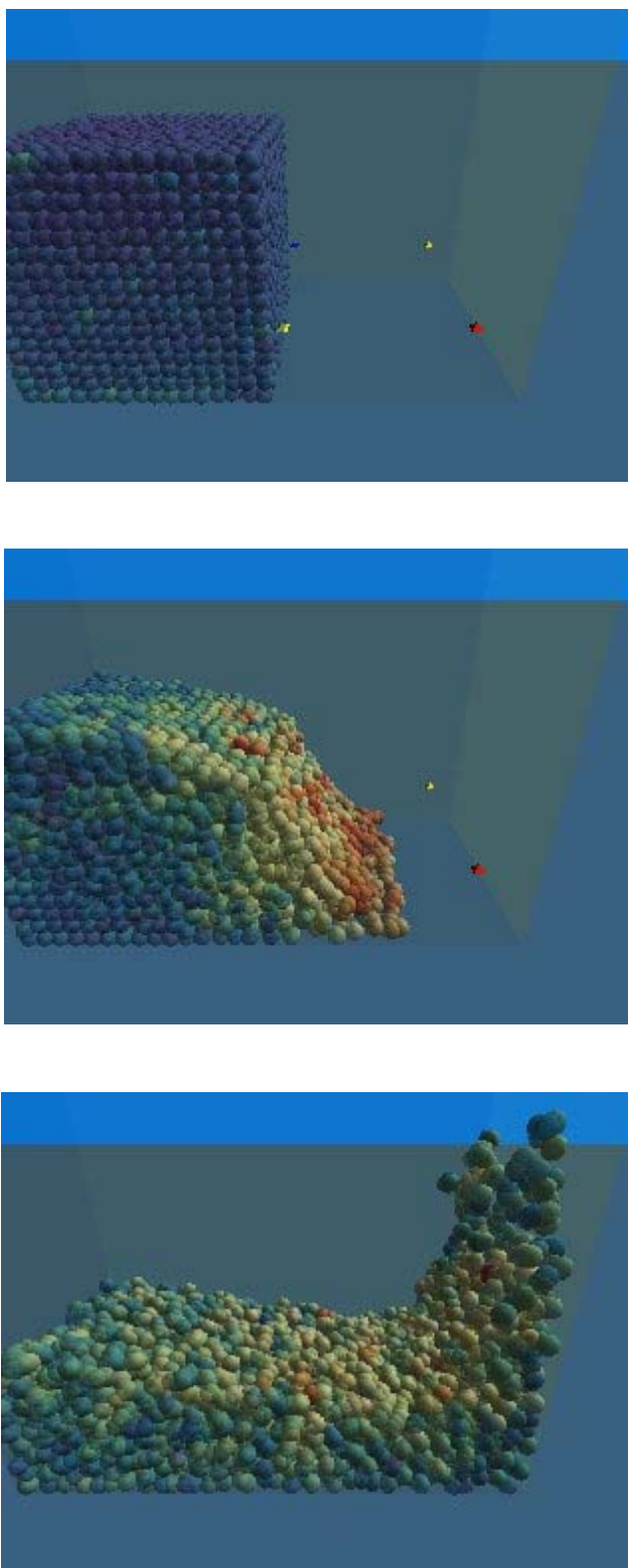
Figure 13: A sequence from a damn break problem at 0.5 second intervals calculated using the Odessa code and the three-dimensional SPH module

However, one area of hydrodynamics in which SPH does not offer any specific advantage, and in fact is definitely not the most appropriate solution technique, occurs in simulations where viscous forces are the dominant factors in determining the nature of the flow. Examples of this type of application include the calculation of lift and drag forces on submerged bodies in high Reynolds number flows. In these applications the flow is highly turbulent and the general features of the flow are determined by the detachment of the boundary layer. The dynamics of this are highly dependent on the viscosity of the fluid. SPH can model drag forces successfully, as the papers by Takeda et al. [74] and Morris et al. [62] have shown, but only for very low Reynolds number flows which are essentially laminar and where the boundary layer can be resolved by the SPH particles. In applications where the Reynolds number is of the order of a million or higher the thickness of the boundary layer is several orders of magnitude smaller than the typical length scale. This causes significant problems for any numerical solution technique because of the need to resolve length scales over several orders of magnitude. An SPH code with a variable smoothing length could certainly be applied to such problems, but would currently offer no specific advantages over traditional grid based methods.

The other area where SPH has had a significant impact in an area of science relevant to defence is in the simulation of the brittle fracture of solids. This is because the sophisticated fracture mechanics models used to accurately simulate the behaviour of these materials requires the entire stress history of a given piece of material. This is easily done using Lagrangian codes because in this approach the frame of reference is attached to the material. Lagrangian methods however suffer from the problem of grid entanglement and become impractical to use in many applications of defence interest. The ability to replace entangled Lagrangian nodes with disconnected SPH particles, as discussed in section 4.0, means that the Lagrangian approach can now still be applied, even in cases of extreme material distortion. As noted in section 5.3, several commercial codes now contain this technique for fracture mechanics modelling and this offers a significantly improved capability for the simulation of ballistic impact on confined and unconfined ceramic targets and transparent armour.

7. Acknowledgements

8. References

1. Balsara, D.S., "von Neumann Stability Analysis of Smoothed Particle Hydrodynamics – Suggestions for Optimal Algorithms", *Journal of Computational Physics*, **121**, 357-372, (1995).

2. Benz, W. "Applications of Smoothed Particle Hydrodynamics (SPH) to Astrophysical Problems", *Computer Physics Communications*, **48**, 97-105, (1988).

3. Benz, W., "Smooth Particle Hydrodynamics: A Review", *Harvard-Smithsonian Center for Astrophysics*, Preprint No. 2884, (1989).

4. Benz, W. and Asphaug, E. "Simulations of Brittle Solids using Smooth Particle Hydrodynamics", *Computer Physics Communications*, **87**, 253-265, (1995).

5. Cartwright, B, Groenenboom, P.H.L, and McGuckin, D., "Examples of Ship Motion and Wash Predictions by Smoothed Particle Hydrodynamics (SPH)", presented at the *9th Symposium on Practical Design of Ships and Other Floating Structures*, Luebeck-Travemuende, Germany, 2004.

6. Cartwright, B., McGuckin, D., Turner, T. and Cannon, S., "The Modelling of Landing Craft Motions inside a flooded Well Dock using Smoothed Particle Hydrodynamics", presented at *Pacific 2006*, Sydney, Australia 2006.

7. Cartwright, B, Xia, J., Cannon, S., McGuckin, D. and Groenenboom, P., "Motion Prediction of Ships and Yachts by Smoothed Particle Hydrodynamics", presented at the *2nd High Performance Yacht Design Conference*, 14-16 February, Auckland, New Zealand, 2006.

8. Cleary, P.W., "Modelling confined multi-material heat and mass flows using SPH", *Applied Mathematical Modelling*, **22**, 981-993 (1998).

9. Cleary, P., Ha, J., Alguine, V and Nguyen, T., "Flow modelling in casting processes", *Applied Mathematical Modelling*, **26**, 171-190 (2002).

10. Clegg, R.A., Sheridan, J., Hayhurst, C.J. and Francis, N.J., "The Application of SPH Techniques in AUTODYN-2D to Kinetic Energy Penetrator Impacts on Multi-Layered Soil and Concrete Targets", *8th International Symposium on Interaction of the Effects of Munitions with Structures*, Virginia, USA, 22-25 April, 1997.

11. Colagrossi, A. and Landrini, M, "Numerical simulation of interfacial flows by smoothed particle hydrodynamics", *Journal of Computational Physics*, **191**, 448-475 (2003)

12. Cole, R.H., *Underwater Explosions*, Princeton, NJ, Princeton University Press, (1948).

13. Corrignan, P. "Analyse Physique des Phénomènes Associés au Ballotement de Liquide dans des Réservoirs (Sloshing)", Ph.D. thesis, Ecole Centrale de Nantes, Novembre 1994.

14. Delorme, L., Souto Iglesias, A. and Abril Pérez, S., "Sloshing loads simulation in LNG tankers with SPH", International Conference on Computational Methods in Marine Engineering, MARINE 2005, Barcelona.

15. De Vuyst, T., Vignjevic, R. and Campbell, J.C., "Coupling between meshless and finite element methods", *International Journal of Impact Engineering*, **31**, 1054-1064 (2005)

16. Doring, M., Andrillon, Y., Alessandrini, B. and Ferrant, P. "SPH Free Surface Flow Simulation", presented at the *18th International Workshop on Water Waves and Floating Bodies*, Le Croisic, 6th-9th April, 2003.

17. Doring, M., Oger, G., Alessandrini, B. and Ferrant, P., "SPH Simulations of Floating Bodies in Waves", *23rd International Conference on Offshore Mechanics and Arctic Engineering*, June 20-25, 2004, Vancouver, British Columbia, Canada.

18. Durrett, R.E. and Matuska, D.A., "The HULL Code, Finite Difference Solution to the Equations of Continuum Mechanics", *Air Force Armament Laboratory* AFATL-TR-78-125 (1978).

19. Fontaine, E. "On the use of Smoothed Particle Hydrodynamics to model extreme waves and their interactions with a structure", presented at *Rogue Waves 2000*, 29-30 November, Le Quartz, Brest, France.

20. Gingold R. A. and Monaghan, J.J., "Smoothed particle hydrodynamics: Theory and application to non spherical stars". *Mon. Not. Roy. Astron. Soc.*, **181**, 375-389, (1977).

21. Gingold, R.A. and Monaghan, J.J., "Binary fission in damped rotating polytropes", *Mon. Not. Roy. Astron. Soc.*, **184**, 481 499, (1978).

22. Gingold,R.A. and Monaghan, J.J., "A numerical study of the Roche and Darwin problems for polytropic stars", Mon. Not. Roy. Astron. Soc., **188**, 45-58, (1979).

23. Gingold,R.A. and Monaghan, J.J., "Kernel Estimates as a Basis for General Particle Methods in Hydrodynamics", *Journal of Computational Physics*, **46**, 429 – 453, (1982).

24. Gingold R. A. and Monaghan, J.J., *Mon. Not. Roy. Astron. Soc.*, **204**, 715 (1983).

25. Gomez-Gesteira, M and Dalrymple, R.A., "Using a Three-Dimensional Smoothed Particle Hydrodynamics Method for Wave Impact on a Tall Structure", Journal of Waterway, Port, Coastal and Ocean Engineering, **130**, 63-69 (2004).

26. Gomez-Gesteira, M., Cerqueiro, D., Crespo, C. and Dalrymple, R.A., "Green water overtopping analyzed with a SPH model", Ocean Engineering, **32**, 223-238 (2005).

27. Hageman, L.J. et al. "HELP, A Multi-Material Eulerian Program for Elastic-Plastic Flows in Two Space Dimensions and Time", *Systems, Science and Software*, SSS-R-75-2654, 1975.

28. Harlow, F.W. and Welch, J.E. "Numerical calculations of time-dependent viscous incompressible flow of fluid with free surface", *Physics of Fluids*, **8**, 2182-2189 (1965)

29. Hayhurst, C.J., Clegg, R.A., Livingston, I.H. and Francis, N.J. "The Application of SPH Techniques in AUTODYN-2D to Ballistic Impact Problems", *16th International Symposium on Ballistics*, San Francisco, CA, 23-28 September, 1996.

30. Hockney, R.W. and Eastwood, J.W., "Computer simulations using particles", Adam Hilger, New York, (1988).

31. Hoover, W.G., Hoover, C.C. and Merritt, E.C., "Smooth particle applied mechanics: conservation of angular momentum with tensile stability and velocity averaging", *Phys. Rev. E*, **69**, 016702-1-10 (2004)

32. Janzon, B., "Modelling Explosively Formed Penetrators and Shaped Charges on Personal Computers using PC-DYNA2D", *Materials Research Laboratory Technical Report*, MRL-TR-93-28, September 1993.

33. Janzon, B., "Numerical Calculations of Collapse and Jet Data for the MRL 38 mm Shaped Charge using PC-DYNA2D" *Materials Research Laboratory Technical Report*, MRL-TR-93-29, September 1993.

34. Johnson, G. R., Petersen, E. H. and Stryk, R. A. "Incorporation of an SPH option into the EPIC code for a wide range of high velocity impact computations", *International Journal of Impact Engineering*, **14**, 385-394 (1993)

35. Johnson, G. R., "Linking of Lagrangian particle methods to standard finite element methods for high velocity impact computations", *Nuclear Engineering and Design*, **150**, 265-274 (1994)

36. Johnson, G.R., Stryk, G.A. and Beissel, S.R. "SPH for high velocity impact computations", *Computer Methods in Applied Mechanics and Engineering*, **139**, 347-373 (1996)

37. Kamoulakos, A., Przybylowicz, M. and Groenboom, P., "Smoothed Particle Hydrodynamics for Space Debris Impact Simulations – An Approach with the PAM-SHOCK Transient Dynamics Code", *International Workshop in New Models and Numerical Codes for Shock Wave Processes in Condensed Media,* St. Catherine's College, Oxford University, Oxford, UK, September 15-19, 1997

38. Kleefsman, K.M.T., "Water impact loading on offshore structures. – A numerical study", Ph.D. thesis, University of Groningen, 2005.

39. Lacome, J.L., "Smoothed Particle Hydrodynamics Method in LS-DYNA", *3rd LS-DYNA Forum*, Bamberg, Germany, 14-15 October, 2004.

40. Lam, C. and McQueen, D., "Numerical Simulation of the Formation and Penetration of Explosively Formed Projectiles", *Computational Techniques and Applications: CTAC-95*, Eds. R. May and A. Easton, World Scientific, (1996).

41. Libersky, L.D. and Petschek, A.G., "Smoothed particle hydrodynamics with strength of materials", in *Proceedings, The Next Free Lagrange Conf.*, H.Tease, J.Fritts and W.Crowley eds., Springer Verlag, NY, **395**, 248-257 (1991)

42. Libersky, L.D., Petschek, A.G., Carney, T.C., Hipp, J.R. and Allahdadi, F.A., "High Strain Lagrangian Hydrodynamics – A Three-Dimensional SPH Code for Dynamic Material Response", *Journal of Computational Physics*, **109**, 67-75 (1993).

43. Liu, G.R. and Liu, M.B, "Smoothed Particle Hydrodynamics – a mesh free particle method", World Scientific, (2005).

44. Livingston, I.H., Verolme, K. and Hayhurst, C.J., "Predicting the Fragmentation Onset Velocity for Different Metallic Projectiles Using Numerical Simulations", *International Journal of Impact Engineering*, **26**, 453-464 (2001)

45. Lucy, L., "A Numerical Approach to Testing the Fission Hypothesis", *Astronomical Journal*, **82**, 1013-1024 (1977).

46. Martin, J.C. and Moyce, W.J., "An experimental study of the collapse of liquid columns on a rigid horizontal plane", *Philos. Trans. Roy. Soc. London, Ser. A*, **244**, 312-324 (1952)

47. May, D.A. and Monaghan, J.J., "Can a single bubble sink a ship?", *Am. J. Phys.*, **71**, 842-849 (2003)

48. Meuric, O.F.J., Sheridan, J.O., Carroll, C., Clegg, R.A. and Hayhurst, C.J., "Numerical Prediction of Penetration into Reinforced Concrete using a Combined Graid based and Meshless Lagrangian approach", *10th International Symposium On Interaction Effects of Munitions with Structures*, California, May, 2001.

49. Monaghan, J. J. "Why Particle Methods Work", *SIAM Journal on Scientific and Statistical Computing*, **3**, 422-433, (1982).

50. Monaghan, J. J., "Particle methods for hydrodynamics", *Computer Physics Report*, **3**, 71-124, (1985).

51. Monaghan, J. J., "An Introduction to SPH", *Computer Physics Communications*, **48**, 89-96, (1988).

52. Monaghan, J.J., "On the problem of penetration in particle methods, *J. Comput. Phys.*, **82**,1- 5, (1989).

53. Monaghan, J. J., "Smoothed Particle Hydrodynamics", *Annual Review of Astronomy and Astrophysics*, **30**, 543-574, (1992).

54. Monaghan, J. J., "Simulating Free Surface Flows with SPH", *Journal of Computational Physics*, **110**, 399-406 (1994).

55. Monaghan, J. J., "Smoothed Particle Hydrodynamics", *Rep. Prog. Phys.*, **68**, 1703-1759, (2005).

56. Monaghan, J.J, private communication with the authors, August 2006.

57. Monaghan, J. J. and Gingold, R.A., "Shock Simulation by the Particle Method SPH", *Journal of Computational Physics*, **52**, 374-389 (1983).

58. Monaghan, J. J. and Kos, A., "Solitary Waves on a Cretan Beach", *Journal of Waterway, Port, Coastal and Ocean Engineering*, **124**, 145-154 (1999).

59. Monaghan, J. J., Kos, A., and Issa, N., "Fluid Motion Generated by Impact", *Journal of Waterway, Port, Coastal and Ocean Engineering*, **129**, 250-259 (2004).

60. Monaghan, J.J. and Lattanzio, J.C., "A refined particle method for astrophysical problems", *Astron. Astrophys.*, **149**, 135-143, (1985).

61. Morris, J.P., "Analysis of Smoothed Particle Hydrodynamics with Applications", Ph.D. thesis, Department of Mathematics, Monash University, July, (1996).

62. Morris, J.P., Fox, P.J. and Zhu, Y., "Modeling Low Reynolds Number Incompressible Flows Using SPH", *Journal of Computational Physics*, **136**, 214-226 (1997).

63. Nichols, B.D. and Hirt, C.W., *J. Comput. Phys.*, **8**, 434 (1971)

64. Nielsen, K.B., "Numerical Predictions of Green Water Loads on Ships", Ph.D. thesis, Technical University of Denmark, June 2003.

65. Oger, G., Doring, M. Alessandrinin, B. and Ferrant, P., "SPH: Towards the simulation of wave-body interactions in extreme seas", presented at the *18th International Workshop on Water Waves and Floating Bodies*, Le Croisic, 6th-9th April, 2003.

66. O'Grady, H.J.P., Hayhurst, C.J. and Fairlie, G.E., "The Numerical Simulation of Warheads, Impact and Blast Phenomena using AUTODYN-2D and AUTODYN-3D", South African Ballistics Synposium, Stellenbosch, South Africa, November 1996.

67. Osher, S. and Sethian, J.A., "Fronts propagating with curvature-dependent speed: Algorithms based on Hamiltonian-Jacobi formulation", *Journal of Computational Physics*, **79**, 12-49 (1988)

68. Petschek, A.G. and Libersky, L.D., "Cylindrical Smoothed Particle Hydrodynamics" *Journal of Computational Physics*, **109**, 76-83 (1993)

69. Randles, P.W. and Libersky, L.D. "Smoothed Particle Hydrodynamics: Some recent improvements and applications", *Comput. Methods Appl. Mech. Engrg.* **139**, 375-408 (1996)

70. Riffert, H, Herold, H., Flebbe, O and Ruder, H., "Numerical aspects of the smoothed particle hydrodynamics method for simulating accretion discs", *Computer Physics Communications*, **89**, 1-16 (1996)

71. Solaas, F. and Faltinsen, O.M., "Combined numerical and analytical solution for sloshing in two-dimensional tanks of general shape", *Journal of Ship Research*", **41**, No.2, June 1997.

72. Souto Iglesis, A., Pérez Rojas, L. and Zamora Rodríguez, R., "Simulation of anti-roll tanks and sloshing type problems with smoothed particle hydrodynamics", *Ocean Engineering*, **31**, 1169-1192 (2004).

73. Swegle, J.W. and Attaway, S.W., "On the feasability of using smoothed particle hydrodynamics for underwater explosion calculations", *Computational Mechanics*, **17**, 151-168 (1995)

74. Takeda, H, Miyama, S.M. and Sekiya, M., "Numerical Simulation of Viscous Flow by Smoothed Particle Hydrodynamics", *Progress of Theoretical Physics*, **92**, 939-960 (1994)

75. Thornton, D., Lam, C. and Chick, M., "Limpet Mine Damage Effects against Simulated Ship Hull Targets", *Naval Platform Vulnerability/Survivability Technical Workshop*, 21-24 November 1994, HMAS Stirling, Western Australia.

76. Watkins, S.J., Bhattal, A.S., Francis, N., Turner, J.A. and Whitworth, A.P., "A new prescription for viscosity in Smoothed Particle Hydrodynamics", *Astron. Astrophys. Suppl. Ser.*, **119**, 177-187 (1996)

DISTRIBUTION LIST

Smoothed Particle Hydrodynamics:
Applications within DSTO

D.A. Jones and D. Belton

AUSTRALIA

DEFENCE ORGANISATION

No. of copies

Task Sponsor

PSO(CapDev) COMAUSNAVSUBGRP, Stirling	1 Printed

S&T Program

Chief Defence Scientist	1
Deputy Chief Defence Scientist Policy	1
AS Science Corporate Management	1
Director General Science Policy Development	1
Counsellor Defence Science, London	Doc Data Sheet
Counsellor Defence Science, Washington	Doc Data Sheet
Scientific Adviser to MRDC, Thailand	Doc Data Sheet
Scientific Adviser Joint	1
Navy Scientific Adviser	1
Scientific Adviser – Army	1
Air Force Scientific Adviser	1
Scientific Adviser to the DMO	1

Deputy Chief Defence Scientist (Platform & Human Systems)	Doc Data Sheet & Executive Summary
Chief of Maritime Platforms Division	Doc Data Sheet & Distribution List
Chief of Weapons Systems Division	Doc Data Sheet & Distribution List
Research Leader: Mr. Kevin Gaylor	Doc Data Sheet & Distribution List
Research Leader: Dr. Jim Brown	Doc Data Sheet & Distribution List
Research Leader: Dr. Christine Scala	Doc Data Sheet & Distribution List
Research Leader: Dr. Norbert Burman, WSD	Doc Data Sheet & Distribution List
Task Manager: Mr. Brendon Anderson	2 Printed + 1 PDF
Author: Dr. D.A. Jones	1 Printed + 1 PDF
Author: Mr. D. Belton	1 Printed + 1 PDF

Dr. Stuart Cannon	1
Mr.Terry Turner	1
Mr. James Clarkson	1
Dr. John Brett	1
Dr. John Wharington	1
Mr. Royce Smart	1
Dr. Stephen Cimpoeru	1
Dr. Lorenz Drack	1
Mr. David Clarke	1
Dr. Li Chen	1
Mr. John Waschl, WSD	1

DSTO Library and Archives

Library Fishermans Bend	Doc Data Sheet
Library Edinburgh	1 printed
Defence Archives	1 printed
Library, Sydney	Doc Data Sheet
Library, Stirling	Doc Data Sheet
Library Canberra	Doc Data Sheet

Capability Development Group

Director General Maritime Development	Doc Data Sheet
Director General Land Development	1
Director General Capability and Plans	Doc Data Sheet
Assistant Secretary Investment Analysis	Doc Data Sheet
Director Capability Plans and Programming	Doc Data Sheet

Chief Information Officer Group

Head Information Capability Management Division	Doc Data Sheet
Director General Australian Defence Simulation Office	Doc Data Sheet
AS Information Strategy and Futures	Doc Data Sheet
Director General Information Services	Doc Data Sheet

Strategy Executive

Assistant Secretary Strategic Planning	Doc Data Sheet
Assistant Secretary International and Domestic Security Policy	Doc Data Sheet

Navy

Maritime Operational Analysis Centre, Building 89/90 Garden Island Sydney NSW	Doc Data Sheet & Distribution List
Deputy Director (Operations)	
Deputy Director (Analysis)	
Director General Navy Capability, Performance and Plans, Navy Headquarters	Doc Data Sheet
Director General Navy Strategic Policy and Futures, Navy Headquarters	Doc Data Sheet

Air Force

SO (Science) - Headquarters Air Combat Group, RAAF Base, Williamtown NSW 2314	Doc Data Sheet & Executive Summary
Staff Officer Science Surveillance and Response Group	Doc Data Sheet & Executive Summary

Army

Australian National Coordination Officer ABCA (AS NCO ABCA), Land Warfare Development Sector, Puckapunyal	Doc Data Sheet
J86 (TCS Group), DJFHQ	Doc Data Sheet
SO (Science) - Land Headquarters (LHQ), Victoria Barracks NSW	Doc Data Sheet & Executive Summary
SO (Science) - Special Operations Command (SOCOMD), R5-SB-15, Russell Offices, Canberra	Doc Data Sheet & Executive Summary
SO (Science), Deployable Joint Force Headquarters (DJFHQ) (L), Enoggera QLD	Doc Data Sheet

Joint Operations Command

Director General Joint Operations	Doc Data Sheet
Chief of Staff Headquarters Joint Operations Command	Doc Data Sheet
Commandant ADF Warfare Centre	Doc Data Sheet
Director General Strategic Logistics	Doc Data Sheet

Intelligence and Security Group

AS Concepts, Capability and Resources	1
DGSTA, Defence Intelligence Organisation	1
Manager, Information Centre, Defence Intelligence Organisation	1
Director Advanced Capabilities	Doc Data Sheet

Defence Materiel Organisation

Deputy CEO	Doc Data Sheet
Head Aerospace Systems Division	Doc Data Sheet
Head Maritime Systems Division	Doc Data Sheet
Program Manager Air Warfare Destroyer	Doc Data Sheet
Guided Weapon & Explosive Ordnance Branch (GWEO)	Doc Data Sheet
CDR Joint Logistics Command	Doc Data Sheet

OTHER ORGANISATIONS

National Library of Australia	1
NASA (Canberra)	1
Library of New South Wales	1

UNIVERSITIES AND COLLEGES
Australian Defence Force Academy

Library	1
Head of Aerospace and Mechanical Engineering	1
Hargrave Library, Monash University	Doc Data Sheet

OUTSIDE AUSTRALIA

INTERNATIONAL DEFENCE INFORMATION CENTRES

US Defense Technical Information Center	1
UK Dstl Knowledge Services	1
Canada Defence Research Directorate R&D Knowledge & Information Management (DRDKIM)	1
NZ Defence Information Centre	1

ABSTRACTING AND INFORMATION ORGANISATIONS

Library, Chemical Abstracts Reference Service	1
Engineering Societies Library, US	1
Materials Information, Cambridge Scientific Abstracts, US	1
Documents Librarian, The Center for Research Libraries, US	1

INFORMATION EXCHANGE AGREEMENT PARTNERS

National Aerospace Laboratory, Japan	1
National Aerospace Laboratory, Netherlands	1
Mr. Jean-Louis Barillon, France	1 printed
Dr. Elaine Oran, Naval Research Laboratory, Washington, DC	1 printed

SPARES	5 Printed

Total number of copies: 56   Printed: 14   PDF: 42

DEFENCE SCIENCE AND TECHNOLOGY ORGANISATION **DOCUMENT CONTROL DATA**	1. PRIVACY MARKING/CAVEAT (OF DOCUMENT)

| 2. TITLE

Smoothed Particle Hydrodynamics: Applications within DSTO | 3. SECURITY CLASSIFICATION (FOR UNCLASSIFIED REPORTS THAT ARE LIMITED RELEASE USE (L) NEXT TO DOCUMENT CLASSIFICATION)

    Document   (U)
    Title   (U)
    Abstract   (U) |

| 4. AUTHOR(S)

D.A. Jones and D. Belton | 5. CORPORATE AUTHOR

DSTO Platforms Sciences Laboratory
506 Lorimer St
Fishermans Bend Victoria 3207 Australia |

6a. DSTO NUMBER DSTO-TR-1922	6b. AR NUMBER AR-013-764	6c. TYPE OF REPORT Technical Report	7. DOCUMENT DATE October 2006

8. FILE NUMBER 2006/1069741/1	9. TASK NUMBER NAV 03/136	10. TASK SPONSOR CANSG	11. NO. OF PAGES 42	12. NO. OF REFERENCES 76

13. URL on the World Wide Web http://www.dsto.defence.gov.au/corporate/reports/DSTO-TR-1922.pdf	14. RELEASE AUTHORITY Chief, Maritime Platforms Division

15. SECONDARY RELEASE STATEMENT OF THIS DOCUMENT

Approved for public release

OVERSEAS ENQUIRIES OUTSIDE STATED LIMITATIONS SHOULD BE REFERRED THROUGH DOCUMENT EXCHANGE, PO BOX 1500, EDINBURGH, SA 5111

16. DELIBERATE ANNOUNCEMENT

No Limitations

17. CITATION IN OTHER DOCUMENTS	Yes

18. DSTO Research Library Thesaurus

Computational fluid dynamics, Hydrodynamics, Fluid dynamics, Fracture mechanics

19. ABSTRACT
Smoothed Particle Hydrodynamics (SPH) is a computational technique for the numerical simulation of the equations of fluid dynamics without the use of an underlying numerical mesh. Although originally developed for use in astrophysical gas dynamics, SPH has recently been applied to many other areas of numerical fluid dynamics and materials modelling, several of which have particular relevance to defence problems of interest to the DSTO. In this report we review the basics of the method and then describe a simple two-dimensional SPH code for the simulation of incompressible fluid flow. The code is then applied to simple problems such as a dam break, the sloshing of water inside confined volumes, and wave breaking over ships. These examples illustrate both the capabilities of the technique and the relative ease with which the method can treat problems which have previously been considered difficult to solve using traditional methods such as finite difference, finite volume or finite element grid based methods. Further applications of the method are then reviewed, concentrating in particular on the utility of the technique in solid mechanics modelling, and then current applications of SPH within Maritime Platforms Division are described.